Spine

SPINE Volume 36, Number 12, pp 951–957

CERVICAL SPINE

Genetic Differences in the Osteogenic Differentiation Potency According to the Classification of Ossification of the Posterior Longitudinal Ligament of the Cervical Spine

Hitoshi Kudo, MD,* Ken-Ichi Furukawa, PhD,† Toru Yokoyama, MD, PhD,§ Atsushi Ono, MD, PhD,* Takuya Numasawa, MD, PhD,* Kanichiro Wada, MD, PhD,* Sunao Tanaka, MD,* Toru Asari, MD,* Kazumasa Ueyama, MD, PhD,‡ Shigeru Motomura, MD, PhD,† and Satoshi Toh, MD, PhD,*

Study Design. We categorized the four types of ossification of the posterior longitudinal ligament (OPLL) of the cervical spine into two groups. We biochemically investigated the genetic differences in the osteogenic differentiation potency between the two groups.

Objective. To investigate the genetic differences in the osteogenic differentiation potency according to the OPLL classification.

Summary of Background Data. Clinical studies on OPLL have revealed that the risk of progression of the ossification area is greatest for continuous and mixed type OPLL. However, until now, these four types of OPLL have been studied as a single condition.

Methods. We categorized the four types of OPLL into the OPLL continuous (continuous or mixed type) and OPLL segmental groups (segmental or circumscribed type). Paraspinal ligaments were aseptically obtained from OPLL patients during surgery. The fibroblast-like cells that migrated from the explants were used for experiments. The cells were placed in a 60-mm culture dishes for total ribonucleic acid preparation and 12 well microplates for alkaline phosphatase (ALP) activity staining. After cultures reached confluence, the cells were cultured in osteogenic medium. The messenger ribonucleic acid expression of bone morphogenetic protein-2 (BMP-2), osterix, tumor necrosis factor-α-stimulated gene-6, and ALP was analyzed by quantitative real time-polymerase chain reaction. Osteogenic differentiation of fibroblast-like cells was determined by histochemically detecting ALP production.

Results. After osteogenic induction, BMP-2 expression increased in the OPLL continuous and segmental groups. Osterix expression increased in the OPLL continuous group only. Tumor necrosis factor-α-stimulated gene-6 expression was suppressed in the OPLL continuous and segmental groups. ALP expression as well as ALP activity staining was higher in the OPLL continuous group than in the OPLL segmental group.

Conclusion. The study revealed genetic differences in the osteogenic differentiation potency between the OPLL continuous and segmental groups. We propose to distinguish OPLL continuous group from segmental group in biochemical studies on OPLL.

Key words: ossification of the posterior longitudinal ligament (OPLL), classification, spinal ligament, osteogenic differentiation potency, alkaline phosphatase. **Spine 2011;36:951–957**

Ossification of the posterior longitudinal ligament (OPLL) of the spine is characterized by ectopic bone formation in the spinal ligaments. In 1960, Tsukimoto first reported OPLL in Japan, and OPLL is a common disorder among Japanese and other Asian populations.[1] The incidence of OPLL in Japan is approximately 3% (1.8%–4.1%), and the male/female ratio for patients diagnosed with OPLL is 1.96 (1.1–3.0).[2] OPLL causes compression of the spinal cord and leads to various degrees of myelopathy. The typical symptoms of OPLL are sensory and motor disturbances of the upper and lower extremities, abnormal reflexes, hyperresponsive deep reflexes, and bladder-bowel dysfunction. Various degrees of dysfunction, such as precise action and gait disturbance, lead to the restriction of activities involved in daily living and the deterioration of the quality of life.

The occurrence and development of OPLL involve many environmental, systemic, and local factors.[3] Examples of the factors are diet, metabolic or endocrinological background, and mechanical stress. Several groups have identified genetic

From the *Department of Orthopaedic Surgery, Hirosaki University Graduate School of Medicine, Hirosaki, Japan; †Department of Pharmacology, Hirosaki University Graduate School of Medicine, Hirosaki, Japan; ‡Department of Orthopaedic Surgery, Hirosaki Memorial Hospital, Hirosaki, Japan; §Department of Orthopaedic Surgery, Odate Municipal General Hospital, Odate, Japan.

Acknowledgment date: November 20, 2009. Revision date: March 23, 2010. Acceptance date: April 26, 2010.

The manuscript submitted does not contain information about medical device(s)/drug(s).

Institutional and Foundation funds were received in support of this work. No benefits in any form have been or will be received from a commercial party related directly or indirectly to the subject of this manuscript.

Supported in part by Grants-in-Aid from the Ministry of Education, Science, Sports (20590245) and Culture of Japan and the Ministry of Health, Labor and Welfare (200052). Karohji Memorial Aid of Medical Study and Hirosaki University Educational Improvemental Promotional Aid also financially supported the study.

Address correspondence and reprint requests to Ken-Ichi Furukawa, PhD, Department of Pharmacology, Hirosaki University, Graduate School of Medicine, 5 Zaifu-cho, Hirosaki 036-8562, Japan.

DOI: 10.1097/BRS.0b013e3181e9a8a6

susceptibilities to OPLL[4]: Reports suggest an increase in collagen Type VI α 1,[5,6] collagen Type XI α 2,[7,8] nucleotide pyrophosphatase,[9–12] leptin receptor,[10] transforming growth factor-β1,[13–15] promyelotic leukemia zinc finger,[16,17] tumor necrosis factor-α-stimulated gene 6 (TSG-6),[17,18] connective tissue growth factor,[19] prostaglandin I2,[20] and endothelin-1[21] among others.

According to the report of the investigation committee on OPLL of the Japanese Ministry of Public Health and Welfare (now the Japanese Ministry of Health, Labor, and Welfare), OPLL of the cervical spine has been classified into four types by lateral plain radiographs[22,23]: (1) continuous type, which involves a long lesion extending over several vertebral bodies; (2) segmental type, which involves one or several separate lesions behind the vertebral bodies; (3) mixed type, which is a combination of the continuous and segmental types; and (4) circumscribed type, which involves a lesion mainly located posterior to a disc space (Figure 1).

It was reported that patients with mixed or continuous type of OPLL had the greatest risk of progression of the ossification area[24,25] and bleeding[26] after surgery. Until now, these four types of OPLL have been studied as a single condition. No report is available on the genetic differences between the types of cervical OPLL according to the classification. The purpose of this study is to survey genetic differences in the osteogenic differentiation potency according to the classification of cervical OPLL.

MATERIALS AND METHODS

This study was approved by the ethics committee of Hirosaki University Graduate School of Medicine. Informed consent was obtained from each patient.

Clinical Diagnosis

The diagnosis of OPLL or non-OPLL (other cervical diseases not related to ectopic ossification, *i.e.*, cervical spondylotic myelopathy) was before surgery confirmed by spine surgeons using radiographs, computed tomography, and magnetic resonance imaging of the cervical spine. Cases with OPLL were classified into four types: continuous, segmental, mixed, or circumscribed type. We categorized cases into the following three groups: non-OPLL group (cervical spondylotic myelopathy), OPLL segmental group (segmental or circumscribed type OPLL), and OPLL continuous group (continuous or mixed type OPLL) on the basis of previous reports.[24,25] The clinical diagnoses and the spinal ligament tissues used in this study are shown in Tables 1, 2, and 3.

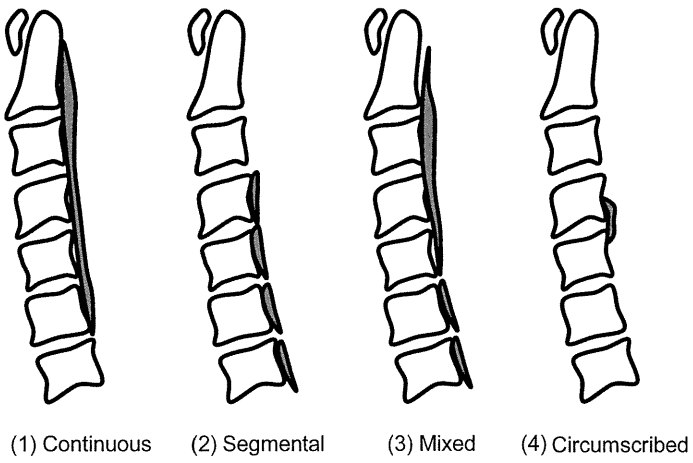

Figure 1. The classification of cervical ossification of the posterior longitudinal ligament. (1) *Continuous type*: a long lesion extending over several vertebral bodies; (2) *segmental type*: one or several separate lesions behind the vertebral bodies; (3) *mixed type*: a combination of the continuous and segmental types; and (4) *circumscribed type*: lesion mainly located posterior to a disc space.

Spinal Ligament Primary Cell Culture

Ligamentum flavum at C3 level was aseptically obtained from OPLL patients during surgery to decompress the spinal cord for myelopathy. As controls, ligamentum flavum at C3 level was obtained from non-OPLL patients during surgery. For cell culture, the ligaments were rinsed with phosphate-buffered saline, after which the surrounding tissue was carefully removed. The ligaments were extirpated carefully from the nonossified site to avoid any possible contamination with osteogenic cells. The collected ligaments were minced into approximately 0.5 mm^3 pieces, washed twice with phosphate-buffered saline, then plated on 100-mm culture dishes, and maintained in Dulbecco's modified Eagle's Medium (DMEM; Nissui Pharmaceutical, Tokyo, Japan) supplemented with 10% heat-inactivated fetal bovine serum (JRH Bioscience, Lenexa, KS), 1% l-glutamine, and 1% penicillin/streptomycin. The explants were incubated in a humidified atmosphere containing 95% air and 5% CO2 at 37°C. The fibroblast-like cells that migrated from the explants were harvested with 0.02% ethylenediaminetetraacetic acid/0.05% trypsin and replated in culture dishes for passage. Fibroblast-like cells were used for experiments after five passages. The tissue collected from each patient is generally small and the cell population migrated from explants is also small. Therefore, it is difficult to use primary cultured cells for any experiment. However, it was confirmed that the morphology and gene expression induced by the osteogenic medium (OSM) did not differ significantly between the second and fifth passage cells.

Chemicals

Dexamethasone was purchased from ICN Biomedicals Inc. (Costa Mesa, CA). All chemicals used in this study were of analytical grade.

Osteogenic Induction

The cells (fifth passage) were placed in a 60-mm culture dishes (2×10^5 cells/dish) for total ribonucleic acid (RNA) preparation. After the cultures reached confluence, the cells were cultured in OSM[27] (DMEM + 1% fetal bovine serum + 0.1 μmol/L dexamethasone) to induce osteogenic differentiation or in the control medium (DMEM + 1% fetal bovine serum) for 24 hours, 48 hours, 3 days, or 7 days.

The cells were then placed in 12 well microplates (0.5×10^5 cells/well) for alkaline phosphatase (ALP) activity

TABLE 1. Non-OPLL Group*

Sample No.	NO-1	NO-2	NO-3	NO-4	NO-5	NO-6	NO-7
Age/sex	74/M	64/M	43/M	76/M	73/M	53/M	78/F
Radiograph	[GRAPHIC]	[GRAPHIC]	[GRAPHIC]	[GRAPHIC]	[GRAPHIC]	[GRAPHIC]	[GRAPHIC]
CT image	[GRAPHIC]	[GRAPHIC]	[GRAPHIC]	[GRAPHIC]	[GRAPHIC]	[GRAPHIC]	[GRAPHIC]

*All patients with cervical spondylotic myelopathy.
CT indicates computed tomographic.

staining. After the cultures reached confluence, the cells were cultured in OSM or in control medium for 3 days or 7 days.

RNA Preparation and Complementary DNA, Synthesis

Total RNA was extracted from cells with QuickGene RNA cultured cell kit S (RC-S) and QuickGene-Mini80 (FUJIFILM Corp., Tokyo, Japan) according to the manufacturer's protocol. The purity and integrity of the total RNA were verified using the RNA 6000 Nano assay with an Agilent Bioanalyzer 2100 (Agilent Technologies, Santa Clara, CA). First strand complementary DNA, was synthesized from 1 μg of total RNA using standard random hexamer priming techniques. The complementary DNAs were stored at −30°C until required.

Real-Time Polymerase Chain Reaction Analysis

Real-time polymerase chain reaction (PCR) was carried out with Power SYBR Green PCR Master Mix on an ABI Prism 7000 Sequence Detection System (Applied Biosystems, Foster City, CA). The conditions for PCR were as follows: 50°C for 2 minutes, 95°C for 10 minutes, and 40 cycles of 95°C for 15 seconds, and 60°C for 1 minute. All samples were analyzed for glycerol 3-phosphate dehydrogenase expression in parallel in the same run. Real-time PCR data were represented as Ct values, where Ct is defined as the cycle number at which the amount of amplified product exceeds the threshold level. The threshold level was configured automatically. To compare the different RNA samples in an experiment, we used the comparative Ct method and compared the RNA expression in samples to that of the control in each experiment. The primers were constructed so that the dynamic range of both the targets and the glycerol 3-phosphate dehydrogenase reference were similar over a wide range of dilutions (1:1 to 1:10,000). Reactions were performed in quadruplet for each cell preparation. Seven independent experiments were performed using cell preparations from 7 non-OPLL patients, 6 OPLL segmental group patients, and 6 OPLL continuous group patients (see Tables 1, 2, and 3). Primers were designed according to the sequences in GenBank using Primer Express (version 1.5) software (Applied Biosystems Foster City, CA), as recommended by the manufacturer, to ensure suitability for use with the ABI Prism 7000 sequence detection system. The sequences of the primers used in this study are shown in Table 4.

ALP Activity Staining

We evaluated osteogenic differentiation of fibroblast-like cells on the basis of ALP production, which was histochemically detected. The cells (OSM for 0 hours, 3 days, or 7 days) were stained using an ALP stain kit (Takara Bio Inc., Shiga, Japan) according to the manufacturer's protocol. The ALP-positive cells stained blue/purple. For each sample, we obtained micrographs of 10 fields for analysis. To evaluate ALP activity staining, the stained area was measured by ImageJ (http://rsb.info.nih.gov/ij/), and the ratio of stained cells to total cells was determined.

Statistical Analysis

The expression of each gene was compared between groups using the ΔΔCt method. Messenger ribonucleic acid (mRNA) expression data were expressed as the mean ± standard error of the mean). mRNA expression was analyzed at the ΔCt stage to exclude potential bias due to averaging of data

TABLE 2. OPLL Segmental Group

Sample No.	OS-1	OS-2	OS-3	OS-4	OS-5	OS-6
Age/sex	70/F	33/M	56/M	82/M	52/M	55/M
Classification	Seg	Seg	Seg	Seg	Cir	Cir
Ossified vertebrae	C5,C6,C7	C4,C5,C6	C4,C5,C6	C5,C6	C5–C6	C6–C7
Other ossified lesion	(+) T4–T7	(–)	(–)	(–)	(–)	(–)
Radiograph	[GRAPHIC]	[GRAPHIC]	[GRAPHIC]	[GRAPHIC]	[GRAPHIC]	[GRAPHIC]
CT image	[GRAPHIC]	[GRAPHIC]	[GRAPHIC]	[GRAPHIC]	[GRAPHIC]	[GRAPHIC]

CT indicates computed tomographic; Seg, segmental type; Cir, Circumscribed type.

TABLE 3. OPLL Continuous Group

Sample No.	OC-1	OC-2	OC-3	OC-4	OC-5	OC-6
Age/sex	50/F	64/M	56/M	54/M	66/M	71/M
Classification	Mix	Mix	Mix	Mix	Mix	Mix
Ossified vertebrae	C2–C4,C5,C6	C2–C4,C5,C6	C2–C3,C4,C5–C6	C2–C4,C6	C3,C5–C7	C2–C4,C5,C6,C7
Other ossified lesion	(+) T1–T3,4–6	(–)	(+)T1–T2	(–)	(+)T4–T6	(–)
Radiograph	[GRAPHIC]	[GRAPHIC]	[GRAPHIC]	[GRAPHIC]	[GRAPHIC]	[GRAPHIC]
CT image	[GRAPHIC]	[GRAPHIC]	[GRAPHIC]	[GRAPHIC]	[GRAPHIC]	[GRAPHIC]

CT indicates computed tomographic; Mix, Mixed type.

transformed through the equation $2^{-\Delta\Delta Ct}$. Data were analyzed by analysis of variance and significant interaction was examined with the Dunnett test for multiple comparisons. ALP staining data were expressed as the mean ± standard error of the mean. Data were analyzed by analysis of variance and significant interactions were further examined with the Tukey test for multiple comparisons. $P < 0.05$ was considered significant.

RESULTS

mRNA Expression of Bone-Related Markers

Bone morphogenetic protein-2 (BMP-2) expression was higher in the OPLL continuous group than in the OPLL segmental and non-OPLL groups in the resting state (0 hours; Figure 2a). After osteogenic induction, BMP-2 expression was further enhanced in the OPLL continuous and segmental groups. At 24 hours of osteogenic induction, BMP-2 expression in the OPLL continuous group was 1.19-fold higher than that in the OPLL segmental group, but not significantly.

The basal level of Osterix expression in the OPLL continuous group was equal to that in the OPLL segmental and non-OPLL groups under the resting state (0 hours) (Figure 2b). After osteogenic induction, Osterix expression was further enhanced in the OPLL continuous group. On the contrary, Osterix expression in the OPLL segmental group and non-OPLL group did not respond to osteogenic induction. At 3 days of osteogenic induction, Osterix expression in the OPLL continuous group was approximately 1.40-fold higher than that in the OPLL segmental group, but not significantly.

TSG-6 has been reported to inhibit osteoblastic differentiation in human mesenchymal stem cells.[17,18] TSG-6 expression in the OPLL continuous and segmental groups was lower than that in the non-OPLL group (Figure 2c). After osteogenic induction, TSG-6 expression was further suppressed in all groups but significantly in OPLL continuous and segmental groups. TSG-6 expression in the OPLL continuous group was almost equal to that in the OPLL segmental group.

ALP expression was higher in the OPLL continuous group than in the OPLL segmental and non-OPLL groups (Figure 2d). After osteogenic induction, ALP expression was further enhanced in all groups, and the expression was higher in the OPLL continuous group than in the OPLL segmental and non-OPLL groups. ALP expression was higher in the OPLL segmental group than in the non-OPLL group.

TABLE 4. mRNA Primers

G3PDH	Forward:	5′-AGATCATCAGCAATGCCTCCTG-3′
	Reverse:	5′-ATGGCATGGACTGTGGTCATG-3′
BMP-2	Forward:	5′-TTAAGATGAAAAGTCTACATGGAAGGTA-3′
	Reverse:	5′-AACTCAACAGTAGCACTGCAAAAAA-3′
Osterix	Forward:	5′-CTGGCTTTCCACAAACTCTCATC-3′
	Reverse:	5′-GGAAGCCGGAGTGCAGGTA-3′
TSG-6	Forward:	5′-GCTACTGGCACATTAGATCAAGTATG-3′
	Reverse:	5′-AAGCAACCTGGGTCATCTTCA-3′
ALP	Forward:	5′-ACGAGCTGAACAGGAACAACGT-3′
	Reverse:	5′-CACCAGCAAGAAGAAGCCTTTG-3′

ALP indicates alkaline phosphatase; BMP-2, bone morphogenetic protein-2; G3PDH, glycerol 3-phosphate dehydrogenase; mRNA, Messenger ribonucleic acid; TSG-6, tumor necrosis factor-α-stimulated gene-6.

ALP Activity Staining

Fibroblast-like cells were histochemically stained for ALP activity to assess osteogenic differentiation. In control samples (OSM for 0 hours), OPLL continuous group and segmental group samples showed more intensive staining than non-OPLL group samples. After osteogenic induction, ALP activity staining increased in OPLL continuous and segmental groups, but not increased in non-OPLL group samples. OPLL continuous group samples showed more intensive staining than OPLL segmental group (Figures 3a, b).

We measured the stained area microscopically (Figure 4a) and estimated the ratio of stained cells to total cells (Figure 4b). The OPLL continuous group samples had significantly larger stained area than the non-OPLL group samples, and they also had larger stained areas than the OPLL segmental group samples. In the control samples, the percentage of stained cells was significantly larger in the OPLL continuous group than in the non-OPLL and OPLL segmental groups. After osteogenic induction, the ratio of stained cells to total cells in the OPLL continuous group significantly increased compared to the ratio in the non-OPLL and OPLL segmental groups.

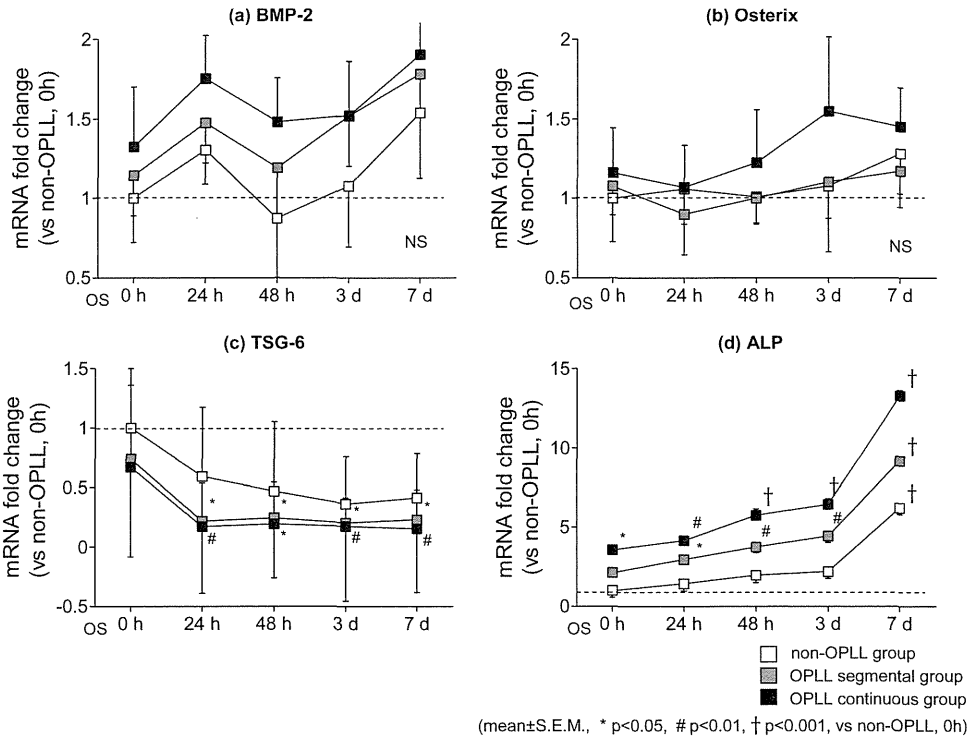

Figure 2. mRNA expression of osteogenic differentiation markers. (a) *BMP-2*: BMP-2 expression in the ossification of the posterior longitudinal ligament (OPLL) continuous group was higher than in the OPLL segmental and non-OPLL groups. (b) *Osterix*: After OS induction, osterix expression in the OPLL continuous group was further enhanced, but Osterix expression in the OPLL segmental and non-OPLL groups did not respond to osteogenic induction. (c) *TSG-6*: TSG-6 expression in the OPLL continuous and segmental groups was lower than in the non-OPLL group. (d) *ALP*: ALP expression in the OPLL continuous group was higher than in the OPLL segmental and non-OPLL groups.

DISCUSSION

It is well known that the ossification area often progresses during the natural course of the disease. Shindo *et al*[28] have reported on the long-term natural course of OPLL. Progression of the ossification was detected in 38% of the segmental type OPLL samples, 75% of the continuous type OPLL samples, and 55% of the mixed type OPLL samples, but it was not related to the aggravation of myelopathy.[28] OPLL often progresses after surgery, which may cause late-onset neurologic deterioration. Kawaguchi *et al*[24] reported the relationship between the progression of OPLL and the clinical results following *en bloc* cervical laminoplasty. Young patients with mixed and continuous types of OPLL had the greatest risk for progression. Some patients had neurologic deterioration following an increase in the thickness of the ossification. Hori *et al*[25] reported the cases of 55 patients who were available for serial radiographs for more than 5 years after cervical laminoplasty. The patients were divided into three groups according to the pattern of OPLL progression.[25] The progression of OPLL was related to the patients' age or OPLL type. As earlier, patients with mixed or continuous types of OPLL had the greatest risk for progression of ossification area.

Sato *et al*[29] reported the histopathological findings of ossified PLL. In the mixed type sample, many hypertrophic chondrocyte-like cells were observed in the calcified cartilaginous area and in the fibrocartilaginous area.[29] In circumscribed type OPLL, the calcified cartilage area was very narrow and the hypertrophic chondrocyte-like cells were fewer than in mixed type OPLL.

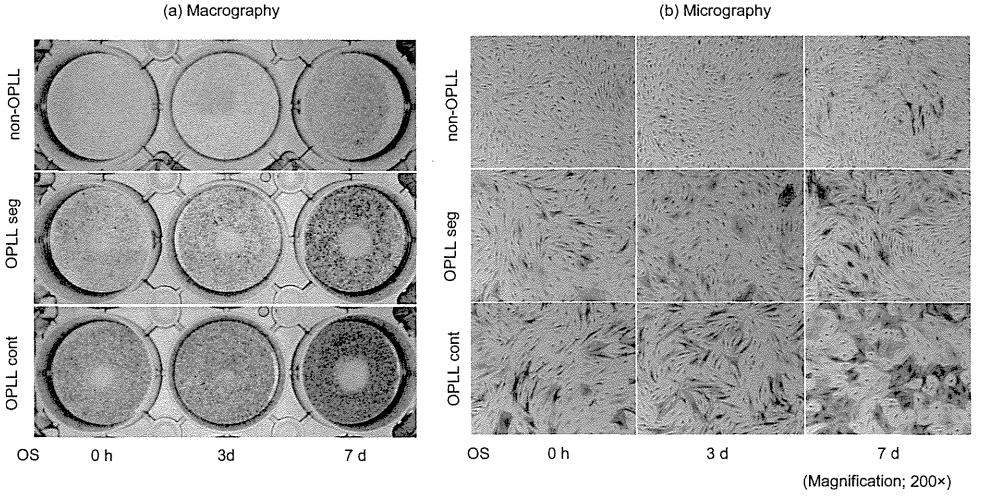

Figure 3. Alkaline phosphatase activity staining. (a) and (b) On macroscopic and microscopic observation, ossification of the posterior longitudinal ligament (OPLL) continuous group and segmental group samples showed more intensive staining than non-OPLL group samples in control samples (0 hours). After osteogenic induction, OPLL continuous group and segmental group samples were more intensively stained than non-OPLL group samples.

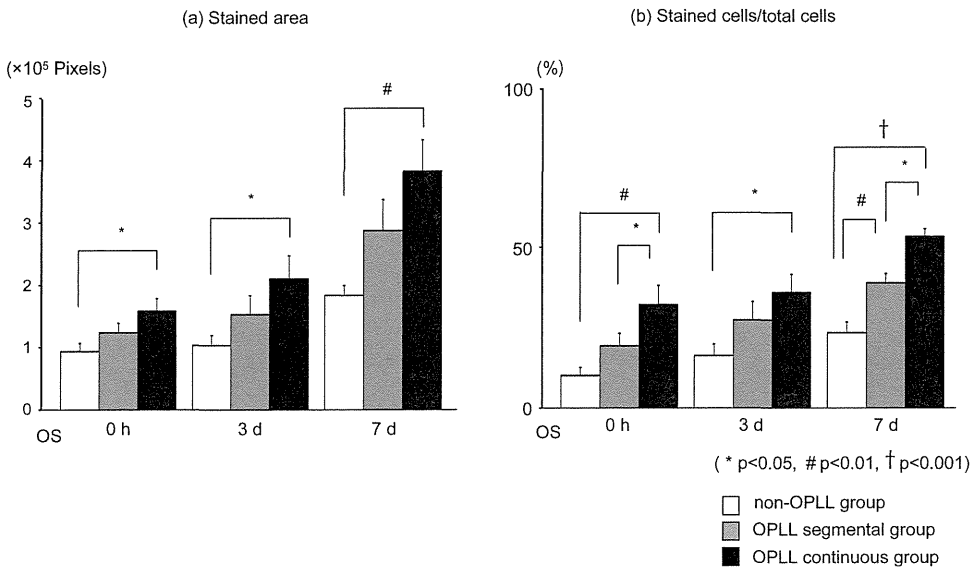

Figure 4. Evaluation of alkaline phosphatase activity staining. (a) and (b) The stained area and ratio of stained cells to total cells was significantly larger in the ossification of the posterior longitudinal ligament (OPLL) continuous group than in the non-OPLL group. The ratio was significantly larger in the OPLL continuous group than in the OPLL segmental group at 0 hours and 7 days.

Clinically and histopathologically, the different features were reported according to the classification for cervical OPLL. However, until now, these four types of OPLL have been studied as one condition. Therefore, on the basis of previous reports, we categorized these four types of OPLL into the OPLL continuous (continuous or mixed type) and OPLL segmental groups (segmental or circumscribed type), and we studied the difference in the osteogenic differentiation potency between the two groups.

It was reported that BMP-2 expression was increased by uniaxial cyclic stretch in OPLL cells, but not in non-OPLL cells.[30] Immunohistochemical studies of mixed-type OPLL tissue revealed significant expression of BMP-2 in the cell soma of mature chondrocytes in the calcified cartilaginous area.[29] In this study, BMP-2 expression was higher in the OPLL continuous group than in the OPLL segmental group before osteogenic induction. After osteogenic induction, BMP-2 expression in the two groups was equal. As in previous reports, BMP-2 was thought to be an important factor in ectopic bone formation of spinal ligament.

About thoracic ossification of the ligamentum flavum, it was reported that Osterix plays an important role in the regulation of ALP activity induced by mechanical stress.[31] Fu *et al*[32] reported that Osterix promoted osteoblast differentiation and mineralization at a heterotopic site.[32] In this study, Osterix expression increased after osteogenic induction in the OPLL continuous group only, and not in the OPLL segmental group and non-OPLL group. Clinically, patients in the OPLL continuous group have a risk of progression of the ossification area; therefore, Osterix may be a key factor for the progression of the ossified area of spinal ligaments.

Tsukahara *et al* identified TSG-6 as a gene that is down regulated during osteoblastic differentiation, and TSG-6 inhibits osteoblastic differentiation induced by the osteogenic differentiation medium.[17,18] In this study, TSG-6 expression in both the OPLL continuous and segmental groups was lower than that in non-OPLL group. Thus, TSG-6 may be a key factor for ectopic bone formation in spinal ligaments, but it may not have any influence on the progression of the ossification area. To reveal the role of TSG-6 in the progression of OPLL requires further investigation such as inhibition of TSG-6 expression by small interfering RNA technique according to OPLL classification.

ALP expression in the OPLL continuous group was higher than that in the segmental group. ALP staining revealed that ALP activity was higher in the OPLL continuous group than in the OPLL segmental group. The cells derived from the OPLL continuous group patients had higher osteogenic differentiation potency than the cells derived from the segmental group patients.

It was reported that segmental or circumscribed type OPLL was transformed to the continuous type in a few cases.[33,34] Whether the OPLL classification is adequate remains controversial. Thus, it is unclear whether the difference in the osteogenic differentiation potency between the OPLL continuous and segmental groups is caused by the natural course of OPLL or by OPLL classification. We do not know whether the patients of the OPLL continuous group in this study really have a high risk of progression of the ossification area and whether patients of the OPLL segmental group in this study have a low risk, because we could not follow-up the patients who provided the tissue samples for long term. And we checked the existence of other ossified lesion. It was revealed that one patient of OPLL segmental group had thoracic lesion, and three patients of OPLL continuous group had thoracic lesion. Not only cervical ossified lesion but other ossified lesion may be important.

We evaluated the genetic differences in the osteogenic differentiation potency on the basis of the OPLL classification. We concluded that the OPLL continuous group cells had higher osteogenic differentiation potency than the OPLL segmental group cells, and the genetic background differed between the OPLL continuous and segmental groups. We propose to distinguish the OPLL continuous group from the OPLL segmental group.

➢ Key Points

- ❑ We categorized the four types of OPLL into the OPLL continuous (continuous or mixed type) and segmental groups (segmental or circumscribed type).
- ❑ We evaluated the osteogenic differentiation potency according to the OPLL classification for the first time.
- ❑ Osteogenic differentiation potency was higher in the OPLL continuous group than in the OPLL segmental group.

Acknowledgments

The authors thank the spine surgery group of the Department of Orthopedic Surgery, Hirosaki University Graduate School of Medicine, and Drs. Yoichi Fujisawa, Hitoshi Sasaki, Taisuke Nitobe, Akio Sannohe, Naoki Echigoya, Koji Tazawa, Takashi Tomita, and Tomoyuki Irie for providing tissue samples.

References

1. Tsukimoto H. A case report-autopsy of syndrome of compression of spinal cord owing to ossification within spinal canal of cervical spines. *Arch Jpn Chir* 1960;29:1003–7.
2. Sakou T, Matsunaga S. Ossification of the posterior longitudinal ligament [In Japanese]. *J Jpn Spine Res Soc* 1996;7:437–48.
3. Furukawa K-I. Pharmacological aspect of ectopic ossification in spinal ligament tissues. *Pharmacol Ther* 2008;118:352–8.
4. Horikoshi T, Maeda K, Kawaguchi Y, et al. A large-scale genetic association study of ossification of the posterior longitudinal ligament of the spine. *Hum Genet* 2006;119:611–6.
5. Tanaka T, Ikari K, Furukawa K-I, et al. Genomewide linkage and linkage disequilibrium analyses identify COL6A1, on chromosome 21, as the locus for ossification of the posterior longitudinal ligament of the spine. *Am J Hum Genet* 2003;73:812–22.
6. Tsukahara S, Miyazawa N, Tanaka T, et al. COL6A1, the candidate gene for ossification of the posterior longitudinal ligament, is associated with diffuse idiopathic skeletal hyperostosis in Japanese. *Spine* 2005;30:2321–4.
7. Maeda S, Koga H, Taketomi E, et al. Functional impact of human collagen alpha2 (XI) gene polymorphism in pathogenesis of ossification of the posterior longitudinal ligament of the spine. *J Bone Miner Res* 2001;16:948–57.
8. Numasawa T, Sakou T, Harata S, et al. Human retinoic X receptor beta: complete genomic sequence and mutation search for ossification of posterior longitudinal ligament of the spine. *J Bone Miner Res* 1999;14:500–8.
9. Yamazaki M, Okawa A, Moriya H. Twy mouse and ossification of the posterior longitudinal ligament of the spine (OPLL). *Clin Calcium* 2002;12:1109–13.
10. Tahara M, Aiba A, Yamazaki M, et al. The extent of ossification of posterior longitudinal ligament of the spine associated with nucleotide pyrophosphatase gene and leptin receptor gene polymorphisms. *Spine* 2005;30:877–80.
11. Okawa A, Nakamura I, Ikegawa S, et al. Mutation in *Npps* in a mouse model of ossification of the posterior longitudinal ligament of the spine. *Nat Genet* 1998;19:271–3.
12. Nakamura I, Ikegawa S, Kawaguchi H, et al. Association of the human *NPPS* gene with ossification of the posterior longitudinal ligament of the spine (OPLL). *Hum Genet* 1999;104:492–7.
13. Kawaguchi Y, Inoue I, Kimura T, et al. Association between polymorphism of the transforming growth factor-beta1 gene with the radiologic characteristic and ossification of the posterior longitudinal ligament. *Spine* 2003;28:1424–6.
14. Kamiya M, Harada A, Yamada Y, et al. Association between a polymorphism of the transforming growth factor-beta1 gene and genetic susceptibility to ossification of the posterior longitudinal ligament in Japanese patients. *Spine* 2001;26:1264–6.
15. Inaba K, Matsunaga S, Ishidou Y, et al. Effect of transforming growth factor-beta on fibroblasts in ossification of the posterior longitudinal ligament. *In Vivo* 1996;10:445–9.
16. Ikeda R, Tanaka H, Furukawa K-I, et al. The promyelotic leukemia zinc finger promotes osteoblastic differentiation of human mesenchymal stem cells as an upstream regulator of CBFA1. *J Biol Chem* 2005;280:8523–30.
17. Inoue I, Ikeda R, Tsukahara S. Current topics in pharmacological research on bone metabolism: Promyelotic leukemia zinc finger (PLZF) and tumor necrosis factor-alpha-stimulated gene 6 (TSG-6) identified by gene expression analysis play roles in the pathogenesis of ossification of the posterior longitudinal ligament. *J Pharmacol Sci* 2006;100:205–10.
18. Tsukahara S, Ikeda R, Inoue I, et al. Tumor necrosis factor α-stimulated gene-6 inhibits osteoblastic differentiation of human mesenchymal stem cells induced by osteogenic differentiation medium and BMP-2. *Biochem J* 2006;398:595–603.
19. Yamamoto Y, Furukawa K-I, Harata S, et al. Possible roles of CTGF/Hcs24 in the initiation and development of ossification of the posterior longitudinal ligament. *Spine* 2002;27:1852–7.
20. Ohishi H, Furukawa K-I, Motomura S, et al. Role of prostaglandin I_2 in the gene expression induced by mechanical stress in spinal ligament cells derived from patients with ossification of the posterior longitudinal ligament. *J Pharmacol Exp Ther* 2003;305:818–24.
21. Iwasawa T, Ueyama K, Motomura S, et al. Pathophysiological role of endothelin in ectopic ossification of human spinal ligaments induced by mechanical stress. *Calcif Tissue Int* 2006;79:422–30.
22. Investigation Committee on OPLL of the Japanese Ministry of Public Health and Welfare. The ossification of the longitudinal ligament of the spine (OPLL). *J Jpn Orthop Assoc* 1981;55:425–40.
23. Yonenobu K, Nakamura K, Toyama Y (Eds.). *OPLL Ossification of the Posterior Longitudinal Ligament.* 2nd ed. Tokyo, Japan: Springer 2006.
24. Kawaguchi Y, Kanamori M, Ishihara H, et al. Progression of ossification of the posterior longitudinal ligament following *en bloc* cervical laminoplasty. *J Bone Joint Surg Am* 2001;83:1798–1802.
25. Hori T, Kawaguchi Y, Kimura T. How does the ossification area of the posterior longitudinal ligament progress after cervical laminoplasty? *Spine* 2006;31:2807–12.
26. Kishiya M, Yokoyama T, Toh S, et al. Comparison of cardiovascular parameters between patients with ossification of posterior longitudinal ligament and patients with cervical spondylotic myelopathy. *J Spinal Disord Tech* 2009;22:361–6.
27. Murata H, Tanaka H, Kawai S, et al. Dexamethasone induces human spinal ligament derived cells toward osteogenic differentiation. *J Cell Biochem* 2004;92:715–22.
28. Shindo S, Nakai O, Yamaura I, et al. Long-term clinical course of ossification the posterior longitudinal ligament in the cervical region [In Japanese]. *Rinsyo Seikeigeka* 2004;39:445–52.
29. Sato R, Uchida K, Baba H, et al. Ossification of the posterior longitudinal ligament of the cervical spine: histopathological findings around the calcification and ossification front. *J Neurosurg Spine* 2007;7:174–83.
30. Tanno M, Furukawa K-I, Motomura S, et al. Uniaxial cyclic stretch induces osteogenic differentiation and synthesis of bone morphogenetic proteins of spinal ligament cells derived from patients with ossification of the posterior longitudinal ligaments. *Bone* 2003;33:475–84.
31. Fan D, Chen Z, Shang Y, et al. Osterix is a key target for mechanical signals in human thoracic ligament flavum cells. *J Cell Physiol* 2007;211:577–84.
32. Fu H, Doll B, Hollinger JO, et al. Osteoblast differentiation *in vitro* and *in vivo* promoted by Osterix. *J Biomed Master Res* 2007;83A:770–8.
33. Chiba K, Yonenobu K, Toyama Y, et al. Multicenter study investigating the postoperative progression of ossification of the posterior longitudinal ligament in the cervical spine: a new computer-assisted measurement. *J Neurosurg Spine* 2005;3:17–23.
34. Taketomi E . Progression of ossification of the posterior longitudinal ligament in the cervical spine. *J Jpn Spine Res Soc* 1997;8:359–66.

Calcif Tissue Int
DOI 10.1007/s00223-010-9456-y

ORIGINAL RESEARCH

P2Y1 Transient Overexpression Induced Mineralization in Spinal Ligament Cells Derived from Patients with Ossification of the Posterior Longitudinal Ligament of the Cervical Spine

Sunao Tanaka · Hitoshi Kudo · Toru Asari · Atsushi Ono · Shigeru Motomura · Satoshi Toh · Ken-Ichi Furukawa

Received: 30 July 2010 / Accepted: 12 December 2010

Abstract Ossification of the posterior longitudinal ligament of the spine (OPLL) is characterized by ectopic bone formation in the spinal ligaments. We previously reported that P2 purinoceptor Y1 (P2Y1) expression is elevated in the spinal ligament cells of OPLL patients, but the role of P2Y1 in the spinal ligament calcification process is unknown. To verify the hypothesis that P2Y1 expression causes ossification of the spinal ligaments, we forced expression of P2Y1 in spinal ligament cells obtained from OPLL and non-OPLL patients using a cytomegaloviral vector. The expression of mRNA and protein was investigated by quantitative real-time polymerase chain reaction and immunofluorescence staining, respectively. After transfection, bone morphogenetic protein-2 (BMP-2) and Sox9 mRNA expression was significantly increased in spinal ligament cells derived from OPLL patients (4.36- and 6.44-fold, respectively) compared with cells from non-OPLL patients (0.57- and 3.64-fold, respectively) 2 days after P2Y1 transient transfection. Furthermore, a statistically significant correlation was observed between BMP-2 and P2Y1 mRNA expression levels in cells obtained from OPLL patients but not from non-OPLL patients. Immunofluorescence analysis showed that BMP-2 and P2Y1 expression was increased in OPLL patients only, while Sox9 expression was increased in OPLL and non-OPLL patients. MRS2279, a selective P2Y1 antagonist, blocked the upregulation of Sox9 and BMP-2 after forced expression of P2Y1. Furthermore, 4 days after transient transfection of P2Y1, mineralization was observed only in spinal ligament cells from OPLL patients. These results suggest that P2Y1 expression plays an important role in ectopic bone formation in the spinal ligaments of OPLL patients.

Keywords Ossification of the posterior longitudinal ligament of the spine (OPLL) · Purinoceptor · Ectopic bone formation · Mineralization

Ossification of the posterior longitudinal ligament of the spine (OPLL) is characterized by ectopic bone formation in the spinal ligament. Ossified ligaments compress the spinal cord and its roots, leading to neurological symptoms. In severe cases, cervical spinal cord compression can cause serious neurological damage including quadriplegia. OPLL is a common disease among Japanese and other Asian populations [1]. Previous reports have revealed that OPLL is associated with genetic factors, dietary habits, and metabolic abnormalities [2–5]; but the underlying pathogenesis is unclear. Spinal cord decompression surgery is often used to relieve symptoms in OPLL patients, but progression of the ossified area may sometimes cause late neurological deterioration [6]. Development of a safe and effective drug therapy is required for this condition.

Immunofluorescence studies have revealed that bone morphogenetic protein (BMP)-2 and tumor necrosis factor (TNF)-β are expressed near the ossified area [7, 8], but the

The authors have stated that they have no conflict of interest.

S. Tanaka · S. Motomura · K.-I. Furukawa (✉)
Department of Pharmacology, Hirosaki University Graduate School of Medicine, 5 Zaifu-cho, Hirosaki, Aomori 036-8562, Japan
e-mail: furukawa@cc.hirosaki-u.ac.jp

S. Tanaka · H. Kudo · T. Asari · A. Ono · S. Toh
Department of Orthopedic Surgery, Hirosaki University Graduate School of Medicine, 5 Zaifu-cho, Hirosaki, Aomori 036-8562, Japan

Published online: 06 January 2011

mechanism underlying the production of these cytokines is unknown. We have previously reported that spinal ligament cells from OPLL patients (OPLL cells) subjected to uniaxial cyclic stretch were induced to express osteogenic genes, such as BMP-2 [9], prostaglandin I_2 synthase [10], Runx2/Cbfa1 [11], and endothelin-1 [12]. In contrast, spinal ligament cells derived from non-OPLL patients (non-OPLL cells) did not respond to uniaxial cyclic stretch. These results suggest that OPLL cells differentiate into osteoblast-like cells in response to mechanical stress.

Mechanical stress has been thought to augment the release of nucleotides in many types of cells, including articular chondrocytes [13], osteoblasts [14], and bone marrow stromal cells [15]. Extracellular nucleotides are believed to interact with two different types of P2 purinoceptors, P2X ligand-gated ion channels and P2Y G protein-coupled receptors. To date, seven subtypes of P2X ($P2X_{1-7}$) and eight P2Y subtypes ($P2Y_{1,2,4,6,11-14}$) have been identified [16–19]. There have been several reports demonstrating that mechanical stress induces osteogenic differentiation in osteoblasts [20, 21] and mesenchymal stem cells [22].

We recently reported that P2 purinoceptors, and especially P2Y1, are expressed at higher levels in spinal ligament cells from OPLL patients than cells from non-OPLL patients [23]. Furthermore, application of uniaxial cyclic stretch to spinal ligament cells from OPLL patients increased their alkaline phosphatase (ALP) mRNA, which was blocked by the selective P2Y1 antagonist [23]. These results indicate that P2Y1 is associated with calcification of the spinal ligament, but it is not known if P2Y1 is directly responsible for ossification of the spinal ligament.

We hypothesize that high-level expression of P2Y1 causes ossification of the spinal ligament. To confirm this hypothesis, we overexpressed P2Y1 in cells from OPLL and non-OPLL patients and investigated the expression of osteogenic marker genes and mineralization of these cells.

Materials and Methods

This study was approved by the Ethics Committee of Hirosaki University Graduate School of Medicine and was conducted according to the principles of the Declaration of Helsinki. Informed consent was obtained from each patient.

Clinical Diagnosis and Spinal Ligament Samples

The diagnosis of OPLL or non-OPLL (cervical spondylotic myelopathy [CSM] or cervical disc herniation [CDH]) was confirmed by X-ray, computed tomography, and magnetic resonance imaging of the cervical spine. Spinal ligament samples were harvested aseptically from the C3 level during cervical surgery. The clinical diagnoses and features of the samples used in this study are shown in Table 1.

Table 1 Clinical diagnosis, gender, and age of patients in this study

Non-OPLL			OPLL		
Code	Diagnosis	Sex/age (years)	Code	Diagnosis	Sex/age (years)
N-1	CSM	M/74	O-1	OPLL	M/70
N-2	CSM	M/55	O-2	OPLL	M/70
N-3	CSM	M/69	O-3	OPLL	F/72
N-4	CDH	M/46	O-4	OPLL	F/50
N-5	CDH	F/72	O-5	OPLL	M/56
N-6	CSM	M/64	O-6	OPLL	M/76
N-7	CSM	M/48	O-7	OPLL	M/69
N-8	CSM	M/53	O-8	OPLL	M/64
N-9	CSM	M/45	O-9	OPLL	M/71
N-10	CSM	F/79	O-10	OPLL	M/43
N-11	CSM	M/66	O-11	OPLL	M/62
N-12	CSM	F/70	O-12	OPLL	M/33
N-13	CSM	F/73	O-13	OPLL	M/53
N-14	CSM	F/72	O-14	OPLL	M/66
			O-15	OPLL	M/71
			O-16	OPLL	M/66
			O-17	OPLL	M/58
			O-18	OPLL	F/70

CSM Cervical spondylotic myelopathy; *CDH* cervical disc herniation; *OPLL* ossification of the posterior longitudinal ligament of the spine; *M* male; *F* female

Cell Culture

Spinal ligament tissues were rinsed with phosphate-buffered saline (PBS) to remove blood and debris, after which the surrounding tissue and calcification area was carefully removed under a dissecting microscope. Collected ligaments were minced into about 0.5-mm^3 pieces and washed twice with PBS, then plated in 100-mm gelatin-coated culture dishes (Asahi Glass, Tokyo, Japan) maintained in conditioned medium, which consisted of Dulbecco's modified Eagle medium (DMEM) containing 10% fetal bovine serum, 1% L-glutamine, 100 units/ml of penicillin G sodium, and 100 μg of streptomycin sulfate; and cultured in a humidified atmosphere of 95% air and 5% CO_2 at 37°C until the growth of adherent cells reached subconfluence. The medium was replaced with fresh medium every 2–3 days. Cells were harvested for passage using 0.02% EDTA/0.05% trypsin. In the present study, spinal ligament cells were used at passages 3–5.

Transient Transfection of P2Y1 into Spinal Ligament Cells

Full-length human P2Y1 cDNA, which is driven by a CMV promoter, was obtained from the TrueClone® collection (OriGene Technologies, Rockville, MD). Cells (2.0×10^5) were seeded into 35-mm gelatin-coated culture dishes (Asahi Glass), and experiments were started after cells reached 80% confluence (day 0). Transient transfection of P2Y1 was performed according to the manufacturer's protocol. Briefly, 0.16 μg of cDNA was added into 50 μl of serum-free DMEM without antibiotics, and 8 μl of SuperFect Transfection Reagent (Qiagen, Santa Clarita, CA) was added to this mixture. After washing cells with warmed PBS, the transfection mixture was added to the dish with 350 μl of conditioned medium. After 3 h of incubation at 37°C in a 5% CO_2 incubator, cells were washed with PBS and the medium was replaced with 2 ml of conditioned medium. As a control, spinal ligament cells derived from the same patients were seeded into another 35-mm dish at the same time as the overexpression culture. The medium was changed every 2–3 days. RNA extractions were performed on days 2 and 6 and alizarin red S staining was performed on day 6.

Total RNA Extraction and cDNA Synthesis

Total RNA was extracted using a QuickGene-mini 80 (Fujifilm, Tokyo, Japan) according to the manufacturer's protocol. RNA concentration was measured using the NanoDrop® ND-1000 (Thermo Scientific, Waltham, MA). After resuspending the purified total RNA in RNase-free water, aliquots containing 1 μg of total RNA were used as a template for the reverse-transcription reaction. Reverse transcription was carried out in a 12-μl reaction mixture containing 1 μg of total RNA, 100 ng of random primer, and 10 nmol of dNTP mix. After 5 min at 65°C, the reaction mixture was cooled on ice for 2 min, and 200 U of M-MLV reverse transcriptase, 200 mmol of DTT, and 10 U of ribonuclease inhibitor were added to the reaction mixture. Primer extension was carried out at 37°C for 60 min and then at 75°C for 15 min.

Quantitative Real-Time PCR

For real-time PCR, the total reaction volume was adjusted to 26 μl and contained 3 μl of a 1:4 dilution of the first-strand reaction product, 1 μl of 10 μM specific forward and reverse primers, 8 μl of pure water, and 13 μl of SYBR green (Applied Biosystems, Foster, CA). Amplification and analysis of cDNA fragments were carried out using an ABI Prism® 7000 (Applied Biosystems). The primers used for this experiment were glyceraldehyde 3-phosphate dehydrogenase (G3PDH), P2Y1, BMP-2, Sox9, Osterix, ALP, and COL1A1, which were designed using Primer Express (version 1.5) software (Applied Biosystems). The primer sequences were as follows: G3PDH (forward, 5′-AGA TCA TCA GCA ATG CCT CCT G-3′; reverse, 5′-ATG GCA TGG ACT GTG GTC ATG-3′), P2Y1 (forward, 5′-TGT GGT GTA CCC CCT CAA GTC CC-3′; reverse, 5′-ATC CGT AAC AGC CCA GAA TCA GCA-3′), BMP-2 (forward, 5′-AGA TGA ACA CAG CTG GTC ACA GA-3′; reverse, 5′-GGA AGG ATG CCC TTT TCC A-3′), Sox9 (forward, 5′-GTA CCC GCA CTT GCA CAA C-3′; reverse, 5′-TCG CTC TCG TTC AGA AGT CTC-3′), Osterix (forward, 5′-CTG GCT TTC CAC AAA CTC TCA TC-3′; reverse, 5′-GGA AGC CGG AGT GCA GGT A-3′), ALP (forward, 5′-ACG AGC TGA ACA GGA ACA ACG T-3′; reverse, 5′-CAC CAG CAA GAA GAA GCC TTT G-3′), COL1A1 (forward, 5′-CCA AAT CTG TCT CCC CAG AA-3′; reverse, 5′-TCA AAA ACG AAG GGG AGA TG-3′). The conditions for PCR were as follows: 95°C for 10 min, 40 cycles at 95°C for 15 seconds, and annealing/primer extension at 60°C for 1 min. All samples were analyzed with G3PDH expression in parallel during the same run. Real-time PCR data were represented as Ct values. To compare the different RNA samples in an experiment, we used the comparative Ct method ($\Delta Ct_{sample} - \Delta Ct_{G3PDH}$). The conversion between ΔΔCt and the relative gene expression level was the fold induction ($2^{-\Delta\Delta Ct}$). The expression levels of each mRNA are represented as the mean ± standard error of the mean, and graphs showing the relative expression levels compared with the control were prepared.

Immunofluorescence Staining

Spinal ligament cells (2.0×10^5) were seeded into a 35-mm glass base dish (Asahi Glass) coated with 1% gelatin. When the cells reached 80% confluence (day 0), the transfection group was overexpressed with P2Y1 according to the method described earlier and immunofluorescence analysis was performed on day 2. Then, 10 nM of MRS 2279, a selective, high-affinity competitive antagonist of the P2Y1 receptor (Tocris Bioscience, Bristol, UK), was added to the indicated groups immediately after transfection with the P2Y1 vector. The glass dish was washed twice with PBS, fixed in 4% (v/v) paraformaldehyde for 30 min, and then rinsed twice with 10% Tween 20 diluted with PBS (TPBS). The glass dish was then filled with 3% skim milk (Wako, Osaka, Japan) for 2 h at room temperature. Primary antibodies consisting of rabbit polyclonal anti-P2Y1 (1:100; Santa Cruz Biotechnology, Santa Cruz, CA) and either mouse polyclonal anti-BMP-2 (1:100, Santa Cruz Biotechnology) or mouse monoclonal anti-Sox9 (1:100; Abnova, Taipei, Taiwan) was added to the

dishes and incubated at 4°C overnight. They were washed three times with TPBS and then incubated with a 1:100 dilution of fluorescein isothiocyanate (FITC)-labeled goat anti-rabbit IgG antibody (Invitrogen, Carlsbad, CA) and goat anti-mouse IgG with DyLight™ 548-conjugated antibody (Rockland Immunochemicals, Gilbertsville, PA) for 2 h at room temperature. Dishes were washed three times with TPBS, and cells were analyzed under a fluorescence microscope (IX71-SIP-FRET; Olympus, Tokyo, Japan).

Alizarin Red S Staining

Four days after P2Y1 transfection (day 6), conditioned medium was aspirated and glass dishes were washed with 2 mL of saline and then fixed with 10% (v/v) formaldehyde for 30 min. After washing three times with pure water, dishes were stained with the alizarin red S solution (2% v/v, pH 4.2) for 5 min and then washed three times with pure water prior to light microscopic examination. Macroscopic and microscopic photographs were then taken.

Statistical Analysis

All data were expressed as means ± S.E.M. The statistical difference of mRNA expression levels between the non-OPLL and OPLL groups was determined using a two-sided paired *t*-test. Differences of $P < 0.05$ were considered to be statistically significant. The relationship between the expression level of P2Y1 mRNA and BMP-2 or Sox9 mRNA was investigated using Pearson's correlation coefficient. All statistical analyses were performed using Excel software (Microsoft, Redmond, WA).

Results

P2Y1 Overexpression Increased BMP-2 and Sox9 Expression of Spinal Ligament Cells Derived from OPLL Patients

To gauge the intrinsic expression levels of P2Y1 and several osteogenic differentiation marker genes, we measured mRNA expression levels using real-time PCR before transfection with P2Y1 (Fig. 1a). OPLL cells expressed higher levels of P2Y1 mRNA than non-OPLL cells. The expression levels of other osteogenic genes, such as BMP-2, Sox9, Osterix, ALP, and COL1A1, were not different between OPLL and non-OPLL cells. Immunofluorescence analysis showed that the spinal ligament cells derived from OPLL patients expressed abundant P2Y1 protein at the surface (Fig. 1b). Forty-eight hours after P2Y1 vector

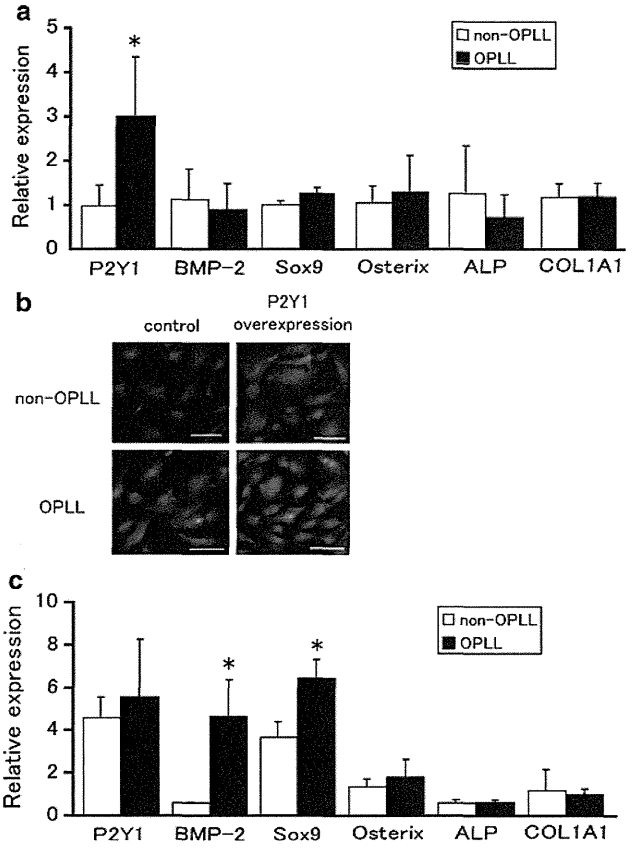

Fig. 1 Expression of P2Y1 and other osteogenic differentiation marker genes. **a** Relative mRNA expression of P2Y1, BMP-2, Sox9, Osterix, ALP, and COLA1 in spinal ligament cells from OPLL ($n = 5$) and non-OPLL ($n = 5$) patients before P2Y1 overexpression. Relative mRNA expression levels of each species were determined on day 0. **b** Immunofluorescence of spinal ligament cells with or without P2Y1 overexpression on day 2. P2Y1 protein was detected using FITC coupled to anti-P2Y1 antibody (*green*). *Scale bar* 100 μm. **c** Relative mRNA expression of P2Y1, BMP-2, Sox9, Osterix, ALP, and COLA1 in spinal ligament cells from OPLL ($n = 5$) and non-OPLL ($n = 5$) patients after P2Y1 overexpression. Relative mRNA expression of each species was determined on day 2 using real-time PCR analysis. * Significantly different from non-OPLL, $P < 0.05$ (Color figure online)

transfection, both OPLL and non-OPLL cells expressed higher levels of P2Y1 (Fig. 1b). Real-time PCR revealed that OPLL cells expressed approximately 5.5-fold higher levels of P2Y1 mRNA after P2Y1 transient transfection and non-OPLL cells expressed approximately 4.6-fold higher levels of P2Y1 mRNA compared with control cells. The increase in BMP-2 and Sox9 mRNA levels in OPLL cells was significantly higher (4.63- and 6.44-fold, respectively) than that in non-OPLL cells (0.57- and 3.64-fold, respectively) (Fig. 1c). P2Y1 mRNA overexpression was specifically related to BMP-2 and Sox9 mRNA expression in OPLL cells. The expression levels of Osterix, ALP, and COL1A1 mRNA, which are often used as early

osteogenic differentiation markers, were not influenced by P2Y1 overexpression in either cell type (Fig. 1c).

P2Y1 mRNA Expression Level Significantly Correlated with the Level of BMP-2 mRNA Expression in Spinal Ligament Cells from OPLL Patients

Overexpression of P2Y1 mRNA induced high levels of BMP-2 mRNA in OPLL cells, but the relationship between P2Y1 mRNA and BMP-2 mRNA expression was unclear. Although the P2Y1 transfection method was performed using the same procedure, there were slight differences in the final expression levels of P2Y1 mRNA between experiments. To confirm the relationship between the expression levels of P2Y1 and BMP-2 mRNAs, the increase (i.e., fold induction) in the level of P2Y1 mRNA was plotted against the increase in the level of BMP-2 mRNA after P2Y1 overexpression. In OPLL cells, a significantly positive correlation was seen between P2Y1 and BMP-2 mRNA ($r = 0.671, P < 0.05$) (Fig. 2b), while in non-OPLL cells, a negative correlation was seen between P2Y1 and BMP-2 mRNA ($r = -0.773$, $P < 0.05$) (Fig. 2a). Furthermore, another 28 transfection experiments using the cells from OPLL patients revealed a very strong correlation between fold inductions of P2Y1 and BMP-2 mRNA ($r = 0.736$, $P < 0.01$) (Fig. 2c). These results suggest that P2Y1 and BMP-2 mRNA expression in spinal ligament cells from OPLL patients are closely related.

P2Y1 Transfection Induces Expression of BMP-2 and Sox9 in OPLL Cells

To confirm that P2Y1 overexpression induces expression of BMP-2 in OPLL cells, we performed dual immunofluorescence staining using anti-P2Y1 antibody and anti-BMP-2 antibody. This analysis demonstrated that P2Y1 transfection induced coexpression of P2Y1 and BMP-2 in OPLL cells (Fig. 3m–o) but not in non-OPLL cells. In non-OPLL cells, BMP-2 protein was only moderately expressed, while P2Y1 was expressed at higher levels (Fig. 3d–f). Furthermore, addition of MRS2279, a highly selective antagonist of P2Y1, reduced the expression of BMP-2 after P2Y1 overexpression in OPLL cells (Fig. 3q, r). These results suggest that P2Y1 overexpression induces expression of BMP-2 only in OPLL cells.

Real-time PCR analysis indicated that P2Y1 overexpression also induces Sox9 mRNA expression in spinal ligament cells derived from both OPLL and non-OPLL cells (Fig. 1c), although the induced levels of Sox9 mRNA were higher in OPLL cells. Immunofluorescence analysis showed that P2Y1 overexpression induced the expression of Sox9 in both OPLL and non-OPLL cells (Fig. 4e, n). Addition of MRS2279 reduced the expression of Sox9 in both OPLL and non-OPLL cells in spite of P2Y1 overexpression (Fig. 4h, q). These results suggest that the expression of Sox9 was induced by P2Y1 overexpression in both OPLL and non-OPLL cells.

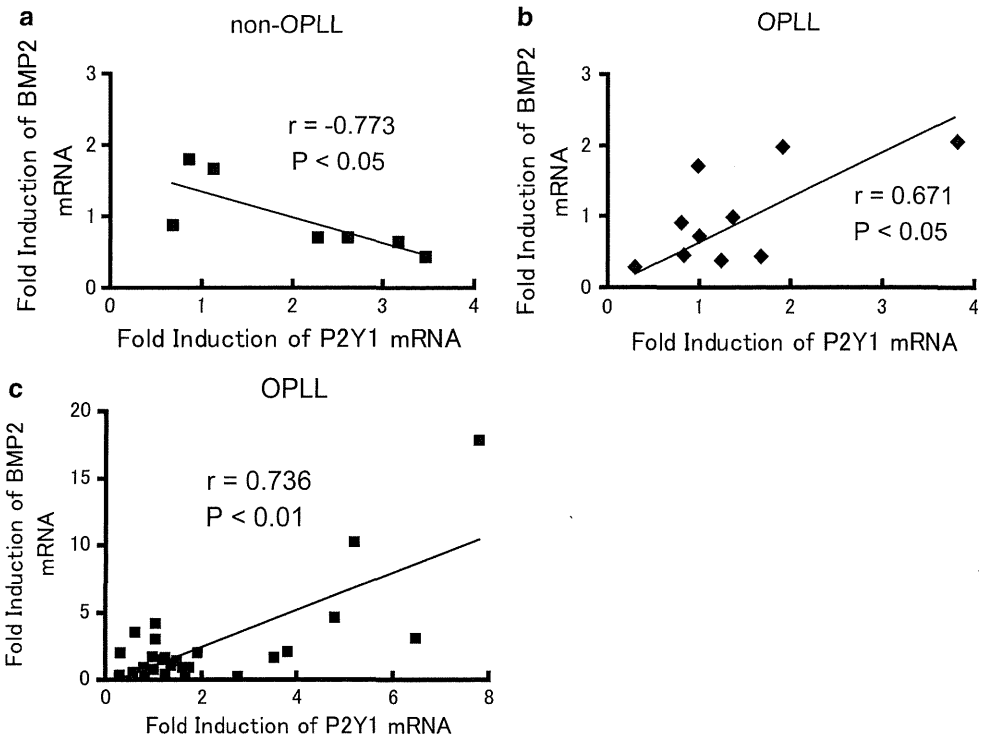

Fig. 2 Correlation analysis of P2Y1 and BMP-2 mRNA expression in spinal ligament cells after P2Y1 transfection. Fold inductions of P2Y1 and BMP-2 mRNA expression in spinal ligament cells 2 days after transfection of the P2Y1 vector are plotted on the x and y axes. **a** Cells derived from non-OPLL patients ($n = 7$). **b** Cells derived from OPLL patients ($n = 10$). **c** Cells derived from OPLL patients ($n = 28$)

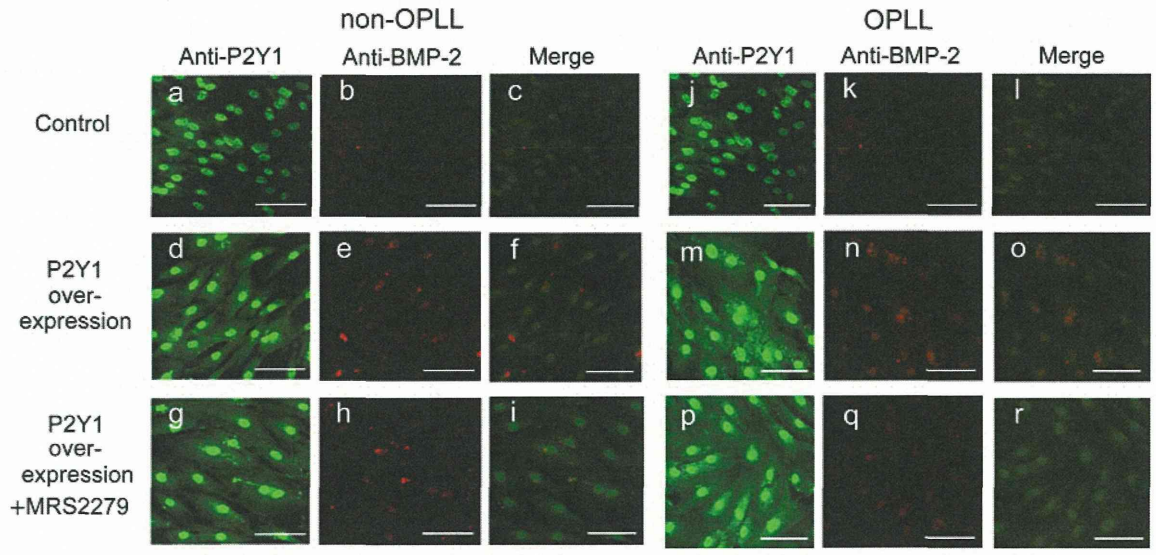

Fig. 3 Immunofluorescence analysis of P2Y1 and BMP-2 expression in spinal ligament cells of OPLL and non-OPLL patients on day 2. P2Y1 or BMP-2 protein was detected using FITC coupled to anti-P2Y1 antibody (**a**, **d**, **g**, **j**, **m**, **p**; *green*) or DyLight 548 coupled to anti-BMP-2 antibody (**b**, **e**, **h**, **k**, **n**, **q**; *red*). In the control group (**a–c**, **j–l**), immunofluorescence was performed on day 2. The P2Y1 overexpression group (**d–f**, **m–o**) was stained 2 days after P2Y1 vector transfection (day 2). In the MRS2279 addition group (**g–i**, **p–r**) 10 nM of MRS 2279 was added immediately after P2Y1 vector transfection (day 0) and immunofluorescence was performed on day 2. Merged images of P2Y1 and BMP-2 staining are shown (**c**, **f**, **i**, **l**, **o**, **r**). *Scale bar* 100 μm (Color figure online)

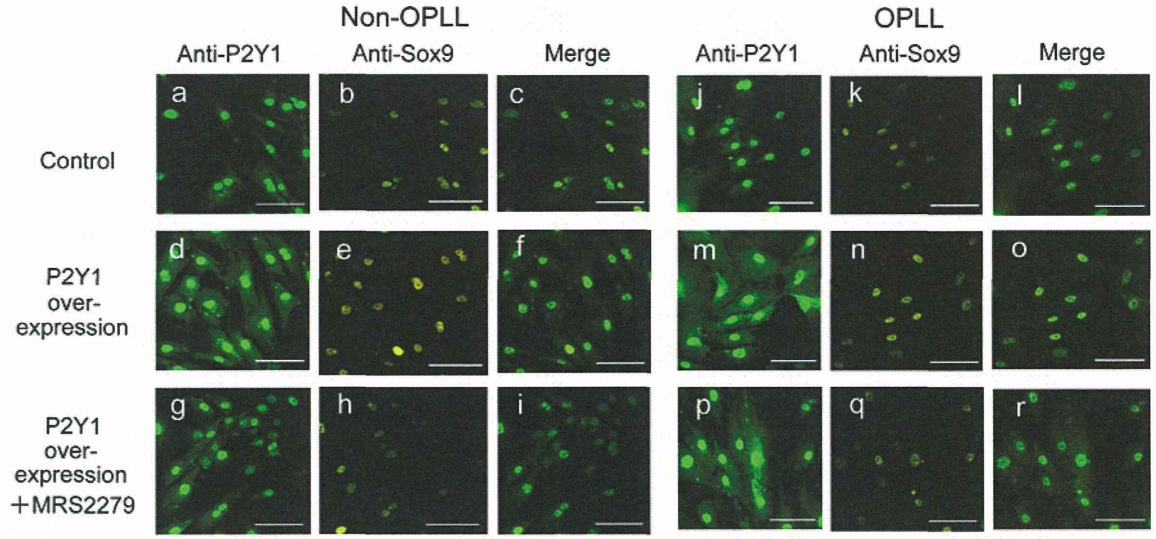

Fig. 4 Immunofluorescence analysis of P2Y1 and Sox9 expression in spinal ligament cells from OPLL and non-OPLL cells on day 2. P2Y1 or Sox9 protein was detected using FITC coupled to anti-P2Y1 antibody (**a**, **d**, **g**, **j**, **m**, **p**; *green*) or DyLight 548 coupled to anti-Sox9 antibody (**b**, **e**, **h**, **k**, **n**, **q**; *yellow*) in non-OPLL (**a–i**) and OPLL (**j–r**) cells. In the control group (**a–c**, **j–l**), immunofluorescence was performed on day 2. The P2Y1 overexpression group (**d–f**, **m–o**) was stained 2 days after P2Y1 vector transfection (day 2). In the MRS2279 addition group (**g–i**, **p–r**) 10 nM of MRS2279 was added immediately after P2Y1 vector transfection (day 0), and immunofluorescence was performed on day 2. Merged images of P2Y1 and Sox9 staining are shown (**c**, **f**, **i**, **l**, **o**, **r**). *Scale bar* 100 μm (Color figure online)

P2Y1 Overexpression Induced Mineralization and an Increase in COL1A1 mRNA Expression in OPLL Cells

Four days after P2Y1 transfection (day 6), alizarin red S staining was performed to investigate mineralization of the spinal ligament cells. The cells derived from non-OPLL patients did not undergo mineralization, even after P2Y1 transfection; but in the cells from OPLL patients, P2Y1 transfection induced mineralization of the extracellular matrix (Fig. 5a, b). Real-time PCR results revealed a significantly higher level of COL1A1 mRNA in P2Y1-transfected OPLL cells compared with non-OPLL cells at day 6 (Fig. 5c).

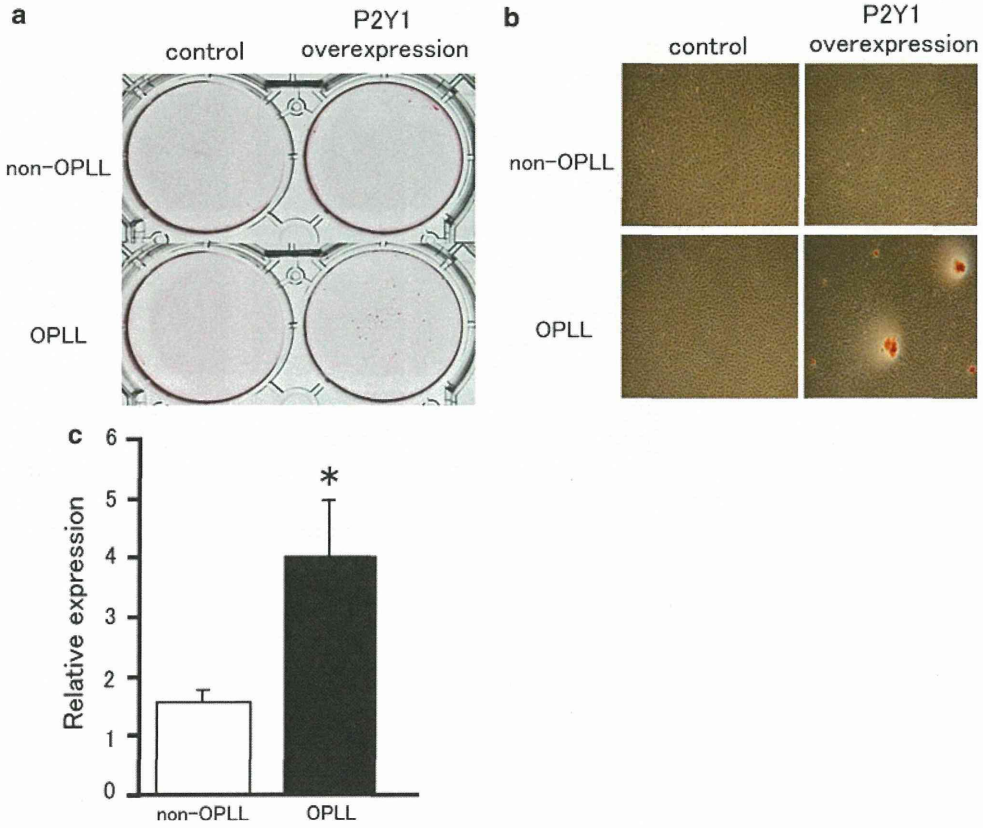

Fig. 5 Alizarin red S staining of spinal ligament cells with or without P2Y1 overexpression. **a** Macroscopic appearance of cell cultures after alizarin red S staining with or without P2Y1 overexpression (at day 6). **b** Microscopic appearance of the same cultures as shown in (**a**) (×16). **c** Real-time PCR analysis of COL1A1 mRNA expression on day 6. The fold increase of COL1A1 mRNA expression after P2Y1 overexpression in OPLL ($n = 4$) and non-OPLL ($n = 4$) cells was compared with control samples. * Significantly different from non-OPLL, $P < 0.05$

Discussion

P2Y1, which belongs to the superfamily of G protein-coupled receptors, has been detected in a variety of mammalian tissues, including endothelium [24], dorsal root ganglion and spinal cord [25], platelet [26], pancreatic β cells [27], and osteoblasts [28]. One of the first cellular responses to extracellular nucleotides is an increase in calcium ion influx [29]. Osteoblasts are reported to respond to extracellular nucleotides during their differentiation and proliferation via P2 purinoceptors [28]. Recently, P2Y1 was reported to be involved in osteoblast proliferation by low-intensity pulsed ultrasound stimulation [30]. Our previous reports have indicated that spinal ligament cells derived from OPLL patients exhibit osteoblast-like characteristics in response to mechanical stimulation [9–12] and that some types of Ca^{2+} channel blockers suppress stretch-induced ALP activity [9]. These cells showed high levels of P2Y1 expression and released adenosine triphosphate (ATP) in response to mechanical stress [23]. We assumed that P2 purinoceptors, especially P2Y1, would be key receptors that activate osteoblastic differentiation of spinal ligament cells in response to mechanical stress.

Our results show that P2Y1 transient overexpression induces the expression of BMP-2 and Sox9 in OPLL cells. To our knowledge, this is the first report that P2 purinoceptors can affect the expression of other genes related to cell differentiation besides BMP-2. We expected that calcification was probably induced in both OPLL and non-OPLL cells via transfection of P2Y1. However, the increase in the level of BMP-2 mRNA was significantly and positively correlated with the P2Y1 mRNA expression level in OPLL cells, while a negative correlation was found in non-OPLL cells. Finally, calcification was observed only in OPLL cells. These results indicate that P2Y1 expression and some reactions to P2Y1 stimulation differ between OPLL and non-OPLL cells and are consistent with our previous report that ATP addition or mechanical stretch increased ALP and osteopontin mRNA expression in cells from OPLL patients but not those from non-OPLL patients [23].

Histological studies have revealed that BMP-2 and Sox9 are highly expressed in the ossification front of the spinal ligament in OPLL patients [7, 8]. BMP-2 is known as a protein that induces ectopic bone formation [31], initiates differentiation of osteoblasts and chondroblasts [32, 33], and induces bone nodule formation in human spinal ligament cells [34]. Furthermore, in spinal ligament cells derived from OPLL patients, osteogenic differentiation is likely to be promoted by rhBMP-2 addition [35]. The process of BMP-2 expression in the spinal ligaments remains unknown. In this study, we found that spinal

ligament cells from OPLL patients express a high level of P2Y1 and that BMP-2 expression is increased after P2Y1 overexpression. Addition of MRS2279, a highly selective antagonist of P2Y1, blocked the increase in BMP-2 expression of OPLL cells after P2Y1 transfection. There was a significant positive correlation between P2Y1 and BMP-2 mRNA expression levels in the OPLL cells. These results suggest that P2Y1 expression induces the production of BMP-2 in OPLL cells.

After forced expression of P2Y1, Sox9 mRNA levels were increased in both OPLL and non-OPLL cells. Immunofluorescence staining showed that this increase was blocked by MRS2279, demonstrating that P2Y1 stimulation induced Sox9. Sox9 is a transcription factor that is essential for chondrogenesis [36]. Previous reports have suggested that Sox9 is expressed downstream of BMP-2 during chondrogenesis [37, 38]. However, other researchers have described that a short hairpin RNA (shRNA) against BMP-2 does not affect the expression of Sox9 [39], suggesting that BMP-2 does not necessarily induce Sox9 expression. Thus, the sequence of BMP-2 and Sox9 expression is still unclear. However, in our experiments, after P2Y1 transfection, BMP-2 was induced only in OPLL cells and Sox9 was induced in both OPLL and non-OPLL cells. These results suggest that P2Y1 overexpression separately stimulates BMP-2 and/or Sox9 expression in OPLL and non-OPLL cells.

Because P2Y1 overexpression led the increase of BMP-2 and Sox9 mRNA in OPLL cells, we consider that P2Y1 overexpression induced osteochondrogenic differentiation of OPLL cells. A recent study reported that overexpression of Sox9 markedly suppressed the expression of ALP in primary chondrocytes [40]. This report suggests that Sox9 expression is important for the early stages of chondrogenesis but that only Sox9 expression cannot mature chondrogenic differentiation. In our study, P2Y1 overexpression induced Sox9 expression in both non-OPLL and OPLL cells but an increase in the level of Sox9 alone failed to induce mineralization in non-OPLL cells. Therefore, expression of both Sox9 and BMP-2 may be required for osteochondrogenesis of spinal ligaments.

Two days after P2Y1 transfection (at day 2), BMP-2 and/or Sox9 mRNA expression levels were increased but levels of ALP and COL1A1 mRNA, which are often used as markers of osteogenic maturation, were not increased, even in OPLL cells. One possible explanation for this is that only the early stage of osteochondrogenic differentiation was observed at this time point. Four days after P2Y1 transfection (at day 6), mineralization was observed and COL1A1 mRNA was expressed at higher levels only in OPLL cells. These results suggest that overexpression of P2Y1 directly induced BMP-2 and Sox9 expression, resulting in osteochondrogenic maturation of OPLL cells.

In conclusion, we observed that P2Y1 transient overexpression induced Sox9 expression in spinal ligament cells from both OPLL and non-OPLL patients but that BMP-2 expression was evident only in cells derived from OPLL patients. P2Y1 overexpression induced mineralization only in cells derived from OPLL patients. These results confirm our hypothesis that P2Y1 is a key receptor that activates calcification of the spinal ligament in OPLL patients. BMP-2 and Sox9 inductions resulting from P2Y1 expression are among the causative factors for ectopic bone formation in the spinal ligament of OPLL patients. P2Y1 inhibitors could therefore have a clinical role to play in blocking calcification of the spinal ligament in OPLL patients.

Acknowledgments The authors acknowledge Drs. Kazumasa Ueyama, Naoki Echigoya, Akio Sannohe, Toshihiro Tanaka, Toru Yokoyama, Takuya Numasawa, Kanichiro Wada, Yoshihito Yamasaki, Tomoyuki Irie, and Taisuke Nitobe for their contributions to sample collection. We also thank Yasuyuki Ishibashi and Kazuhiko Seya of the Hirosaki University Graduate School of Medicine for their valuable suggestions. This work was supported by grants-in-aid from the Health Labour Sciences Research of Japan.

References

1. Trojan DA, Pouchot J, Pokrupa R, Ford RM, Adamsbaum C, Hill RO, Esdaile JM (1992) Diagnosis and treatment of ossification of the posterior longitudinal ligament of the spine. Am J Med 92: 296–306
2. Tanaka T, Ikari K, Furushima K, Okada A, Tanaka H, Furukawa K, Yoshida K, Ikeda T, Ikegawa S, Hunt SC, Takeda J, Toh S, Harata S, Nakajima T, Inoue I (2003) Genomewide linkage and linkage disequilibrium analyses identify COL6A1, on chromosome 21, as the locus for ossification of the posterior longitudinal ligament of the spine. Am J Hum Genet 73:812–822
3. Kobashi G, Washio M, Okamoto K, Sasaki S, Yokoyama T, Miyake Y, Sakamoto N, Ohta K, Inaba Y, Tanaka H (2004) High body mass index after age 20 and diabetes mellitus are independent risk factors for ossification of the posterior longitudinal ligament of the spine in Japanese subjects: a case-control study in multiple hospitals. Spine 29:1006–1010
4. Akune T, Ogata N, Seichi A, Ohnishi I, Nakamura K, Kawaguchi H (2001) Insulin secretory response is positively associated with the extent of ossification of the posterior longitudinal ligament of the spine. J Bone Joint Surg Am 83:1537–1544
5. Furukawa K-I (2008) Pharmacological aspect of ectopic ossification in spinal ligament tissues. Pharmacol Ther 118:352–358
6. Iwasaki M, Kawaguchi Y, Kimura T, Yonenobu K (2002) Long-term results of expansive laminoplasty for ossification of the posterior longitudinal ligament of the cervical spine: more than 10 years follow up. J Neurosurg 96(2 Suppl):180–189
7. Kawaguchi H, Kurokawa T, Hoshino Y, Kawahara H, Ogata E, Matsumoto T (1992) Immunohistochemical demonstration of bone morphogenetic protein-2 and transforming growth factor-β in the ossification of the posterior longitudinal ligament of the cervical spine. Spine 17(3 Suppl):S33–S36
8. Sato R, Uchida K, Kobayashi S, Yayama T, Kokubo Y, Nakajima H, Takamura T, Bangirana A, Itoh H, Baba H (2007) Ossification of the posterior longitudinal ligament of the cervical spine:

histopathological findings around the calcification and ossification front. J Neurosurg Spine 7:174–183
9. Tanno M, Furukawa K, Ueyama K, Harata S, Motomura S (2003) Uniaxial cyclic stretch induces osteogenic differentiation and synthesis of bone morphogenetic proteins of spinal ligament cells derived from patients with ossification of the posterior longitudinal ligaments. Bone 22:475–484
10. Ohishi H, Furukawa K, Iwasaki K, Ueyama K, Okada A, Motomura S, Harata S, Toh S (2003) Role of prostaglandin I_2 in the gene expression induced by mechanical stress in spinal ligament cells derived from patients with ossification of the posterior longitudinal ligament. J Pharmacol Exp Ther 305:818–824
11. Iwasaki K, Furukawa K, Tanno M, Kusumi T, Ueyama K, Tanaka M, Kudo H, Toh S, Harata S, Motomura S (2004) Uni-axial cyclic stretch induces Cbfa1 expression in spinal ligament cells derived from patients with ossification of the posterior longitudinal ligament. Calcif Tissue Int 74:448–457
12. Iwasawa T, Iwasaki K, Sawada T, Okada A, Ueyama K, Motomura S, Harata S, Inoue I, Toh S, Furukawa K (2006) Pathophysiological role of endothelin in ectopic ossification of human spinal ligaments induced by mechanical stress. Calcif Tissue Int 79:422–430
13. Graff RD, Lazerowski ER, Banes AJ, Lee GM (2000) ATP release by mechanically loaded porcine chondrons in pellet culture. Arthritis Rheum 43:1571–1579
14. Romanello M, Pani B, Bicego M, D'Andrea P (2001) Mechanically induced ATP release from human osteoblastic cells. Biochem Biophys Res Commun 289:1275–1281
15. Riddle RC, Taylor AF, Rogers JR, Donahue HJ (2007) ATP release mediates fluid flow-induced proliferation of human bone marrow stromal cells. J Bone Miner Res 22:589–600
16. Ralevic V, Burnstock G (1998) Receptors for purines and pyrimidines. Pharmacol Rev 50:413–492
17. North RA (2002) Molecular physiology of P2X receptors. Physiol Rev 82:1013–1067
18. Burnstock G (2004) Introduction: P2 receptors. Curr Top Med Chem 4:793–803
19. von Kügelgen I (2006) Pharmacological profiles of cloned mammalian P2Y-receptor subtypes. Pharmacol Ther 110:415–432
20. Kanno T, Takahashi T, Tsujusawa T, Ariyoshi W, Nishihara T (2007) Mechanical stress-mediated Runx2 activation is dependent on Ras/ERK1/2 MAPK signaling in osteoblasts. J Cell Biochem 101:1266–1277
21. Liu D, Genetos DC, Shao Y, Geist DJ, Li J, Ke HZ, Turner CH, Duncan RL (2008) Activation of extracellular-signal regulated kinase (ERK1/2) by fluid shear is Ca^{2+}- and ATP-dependent in MC3T3-E1 osteoblasts. Bone 42:644–652
22. Qi MC, Hu J, Zou SJ, Chen HQ, Zhou HX, Han LC (2008) Mechanical strain induces osteogenic differentiation: Cbfa1 and Ets-1 expression in stretched rat mesenchymal stem cells. Int J Oral Maxillofac Surg 37:453–458
23. Sawada T, Kishiya M, Kanemaru K, Seya K, Yokoyama T, Ueyama K, Motomura S, Toh S, Furukawa K (2008) Possible role of extracellular nucleotides in ectopic ossification of human spinal ligaments. J Pharmacol Sci 106:152–161
24. Shen J, DiCorleto PE (2008) ADP stimulates human endothelial cell migration via P2Y1 nucleotide receptor-mediated mitogen-activated protein kinase pathways. Circ Res 102:448–456
25. Kobayashi K, Fukuoka T, Yamanaka H, Dai Y, Obata K, Tokunaga A, Noguchi K (2006) Neurons and glial cells differentially express P2Y receptor mRNAs in the rat dorsal root ganglion and spinal cord. J Comp Neurol 498:443–454
26. Baurand A, Gachet C (2003) The P2Y1 receptor as a target for new antithrombotic drugs: a review of the P2Y1 antagonist MRS-2179. Cardiovasc Drug Rev 21:67–76
27. Léon C, Freund M, Latchoumanin O, Farret A, Petit P, Cazenave JP, Gachet C (2005) The $P2Y_1$ receptor is involved in the maintenance of glucose homeostasis and insulin secretion in mice. Purinergic Signal 1:145–151
28. Orriss IR, Knight GE, Ranasinghe S, Burnstock G, Arnett TR (2006) Osteoblast responses to nucleotides increase during differentiation. Bone 39:300–309
29. Waldo GL, Harden TK (2004) Agonist binding and Gq-stimulating activities of the purified human P2Y1 receptor. Mol Pharmacol 65:426–436
30. Alvarenga EC, Rodrigues R, Caricati-Neto A, Silva-Filho FC, Paredes-Gamero EJ, Ferreira AT (2010) Low-intensity pulsed ultrasound-dependent osteoblast proliferation occurs by via activation of the P2Y receptor: role of the P2Y1 receptor. Bone 46:355–362
31. Wozney JM, Rosen V, Celeste AJ, Mitsock LM, Whitters MJ, Kriz RW, Hewick RM, Wang EA (1988) Novel regulators of bone formation: molecular clones and activities. Science 242: 1528–1534
32. Liu T, Gao Y, Sakamoto K, Minamizato T, Furukawa K, Tsukazaki T, Shibata Y, Bessho K, Komori T, Yamaguchi A (2007) BMP-2 promotes differentiation of osteoblasts and chondroblasts in *Runx2*-deficient cell lines. J Cell Physiol 211:728–735
33. Matsubara T, Kida K, Yamaguchi A, Hata K, Ichida F, Meguro H, Aburatani H, Nishimura R, Yoneda T (2008) BMP2 regulates Osterix through Msx2 and Runx2 during osteoblast differentiation. J Biol Chem 283:29119–29125
34. Moon SH, Park SR, Kim H, Kwon UH, Kim KH, Kim HS, Lee HM (2004) Biologic modification of ligamentum flavum cells by marker gene transfer and recombinant human bone morphogenetic protein-2. Spine 29:960–965
35. Kon T, Yamazaki M, Tagawa M, Goto S, Terakado A, Moriya H, Fujimura S (1997) Bone morphogenetic protein-2 stimulates differentiation of cultured spinal ligament cells from patients with ossification of the posterior longitudinal ligament. Calcif Tissue Int 60:291–296
36. Akiyama H, Chaboissier MC, Martin JF, Schedl A, de Crombrugghe B (2002) The transcription factor Sox9 has essential roles in successive steps of the chondrocyte differentiation pathway and is required for expression of Sox5 and Sox6. Genes Dev 16:2813–2828
37. Zehentner BK, Dony C, Burtscher H (1999) The transcription factor Sox9 is involved in BMP-2 signaling. J Bone Miner Res 14:1734–1741
38. Pan Q, Yu Y, Chen Q, Li C, Wu H, Wan Y, Ma J, Sun F (2008) Sox9, a key transcription factor of bone morphogenetic protein-2-induced chondrogenesis, is activated through BMP pathway and a CCAAT box in the proximal promoter. J Cell Physiol 217:228–241
39. Bais MV, Wigner N, Young M, Toholka R, Graves DT, Morgan EF, Gerstenfeld LC, Einhorn TA (2009) BMP2 is essential for post natal osteogenesis but not for recruitment of osteogenic stem cells. Bone 45:254–266
40. Amano K, Hata K, Sugita A, Takigawa Y, Ono K, Wakabayashi M, Kogo M, Nishimura R, Yoneda T (2009) Sox9 family members negatively regulate maturation and calcification of chondrocytes through up-regulation of parathyroid hormone-related protein. Mol Biol Cell 20:4541–4551

Journal of Biomechanics 44 (2011) 2313–2315

Contents lists available at ScienceDirect

Journal of Biomechanics

journal homepage: www.elsevier.com/locate/jbiomech
www.JBiomech.com

Short communication

Stretch along the craniocaudal axis improves shape recoverability of the spinal cord

Hiroshi Ozawa [a,*], Takeo Matsumoto [b], Toshiro Ohashi [c], Masaaki Sato [d], Eiji Itoi [a]

[a] Department of Orthopaedic Surgery, Tohoku University School of Medicine, 1-1 Seiryomachi, Aobaku, Sendai, 980-8574, Japan
[b] Department of Mechanical Engineering, Nagoya Institute of Technology, Nagoya, Japan
[c] Faculty of Engineering, Hokkaido University, Sapporo, Japan
[d] Graduate School of Biomedical Engineering, Tohoku University, Sendai, Japan

ARTICLE INFO

Article history:
Accepted 15 June 2011

Keywords:
Biomechanics
Shape recoverability
Spinal cord
Stretch
Tensile stress

ABSTRACT

The spinal cord is physiologically stretched along the craniocaudal axis, and is subjected to tensile stress. The purpose of this study was to examine the effect of the tensile stress on morphological plasticity of the spinal cord under compression and decompression condition. The C1–T2 spinal column was excised from 4 rabbits. The laminae and lateral masses were removed. After excision of surrounding structures, a small rod was placed on the spinal cord. The rod was connected with a pan of the scale balance. Varying the weight between 0 and 20 g on the other scalepan, the indentation of the rod was measured. Then, the spinal cord was cut transversely to remove longitudinal tensile stress. The samples were measured again with the same protocol at point 10 mm caudal to each pre-measured point on the spinal cord. The shape recovery rate was calculated. The length of the spinal cord decreased by 9.7% after the separation. The maximum indentation was 2.1 mm (mean) at 20 g, and did not differ between the separated and un-separated cords. The recovery rate was not significantly different between the separated and un-separated cords until 3 g. At the load under 3 g, the recovery rate after the separation was significantly lower than that before the separation. The tensile stress along the craniocaudal axis in the spinal cord did not affect the spinal cord deformation in response to the compression, but it did affect the shape recoverability after the decompression.

1. Introduction

The spinal cord is physiologically stretched along the craniocaudal axis, and is subjected to tensile stress. Breig and el-Nadi (1966) reported that the spinal canal decreases in length when the spine is extended and increases in length when the spine is flexed in human cadavers. The spinal cord adapts to these changes of length by elongating and shortening itself. Tensile stress in the spinal cord is produced by the stretching of the spinal cord.

Clinically, the excess increase or decrease of the tensile stress in the spinal cord induces various pathological conditions. Tethered cord syndrome, especially tight filum terminale, is caused by the pulling of the spinal cord at the base of the spinal canal. The spinal cord is stretched and should present the increase of the tensile stress with growth, leading to progressive spinal cord damage. On the other hand, the decrease of the tensile stress in the spinal cord causes the bending of the spinal cord. It may induce neurologic deterioration as in spinal shortening by vertebral column resection (O'Shaughnessy et al., 2008).

Cervical myelopathy is a well-known spinal cord compression syndrome. It is caused by narrowing of the spinal canal due to degenerative changes in the cervical spine. The spinal cord is deformed according to compression as observed on CT myelograms and axial MR images. The cross-sectional area of the spinal cord decreases in response to compression and increases after decompressive surgery (Ozawa et al., 2004). Biomechanical analysis of the spinal cord is important to clarify the morphological plasticity of the spinal cord. Although various mechanical factors regulating the morphology of the spinal cord have been studied, the influence of physiological tensile stress in the spinal cord has not been studied from the viewpoint of the morphological plasticity. The purpose of this study was to investigate the effect of the tensile stress on the morphology of the spinal cord under compression and decompression in rabbits.

2. Materials and Methods

2.1. Experiments

Animal experiments and treatments were conducted in accordance with the guide for animal experimentation at Tohoku University. Four Japanese rabbits

* Corresponding author. Tel.: +81 22 717 7245; fax: +81 22 717 7248.
E-mail address: hozawa@med.tohoku.ac.jp (H. Ozawa).

0021-9290/$ - see front matter © 2011 Elsevier Ltd. All rights reserved.
doi:10.1016/j.jbiomech.2011.06.017

(mean weight 2600 g, range 2400–2800 g) were killed by intravenous injection of a high dose pentobarbital. The spinal column and cord from C1 to T2 were excised from each rabbit. The specimens were maintained moist with a physiological saline solution during testing. Room temperature was kept at 18 °C.

All tests were accomplished within 40 min after the excision. The laminae and lateral masses between C3 and C7 were removed, and the specimen was put on the flat test table with the vertebral body down. After removal of the posterior half of the dura mater and the arachnoid membrane, the dentate ligaments and anterior and posterior rootlets were carefully dissected between C3 and C7. The spinal cord was not taken out of spinal column. It was confirmed not to adhere to the surrounding structure. A rod of 5 mm in diameter was placed on the midline of the spinal cord. The rod was connected with a pan of a scale balance (Fig. 1). Varying the weight on the other scalepan, the indentation of the rod on the spinal cord was measured as a vertical displacement of the pan using a laser displacement meter (LD-1100S-005, Ono Sokki, Tokyo, Japan) at C3/4 and C5 levels (2 points). The origin of the measurement was taken as the point before applying the load. The load on the spinal cord was increased from 0 to 1, 3, 5, 10, and 20 g, and then decreased to 10, 5, 3, 1, and 0 g at 60 s intervals. The displacement was measured just before the load change. Then, the spinal cord was cut transversely and separated at C2/3 and C7/T1, and the longitudinal tensile stress was removed (Fig. 2). The samples were measured again with the same protocol at 2 points 10 mm caudal to each pre-measured point on the spinal cord so that the residual indentation of the spinal cord caused by the previous measurement did not affect the new measurement.

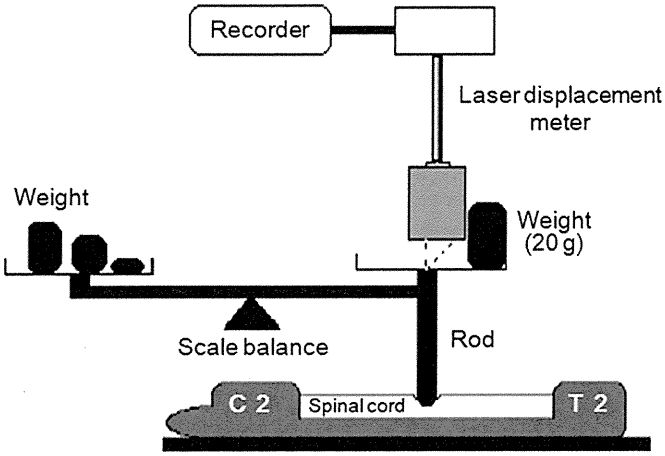

Fig. 1. Schematic drawing of the indentation test of the spinal cord. A rod of 5 mm in diameter was placed on the spinal cord. The rod was connected with a pan of a scale balance. Varying the weight on the other scalepan, the indentation of the rod on the spinal cord was measured with a laser displacement meter as a vertical displacement of the pan.

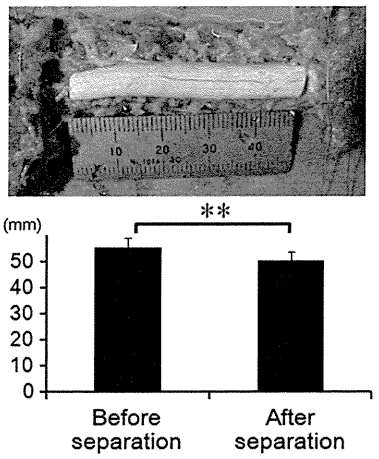

Fig. 2. Change in the spinal cord length. Spinal cord was cut transversely and separated at C2 /3 and C7/T1 to remove the tensile stress. The craniocaudal length of the spinal cord decreased by about 10% (upper picture). The craniocaudal length of the cervical spinal cord after the separation was significantly shorter than the length before the separation (**$p < 0.01$).

The shape recovery rate was defined as the proportion of elastic recovery under unloaded condition to the maximum deformation as follows:

A shape recovery rate (%)=(maximum indentation − residual indentation)/maximum indentation × 100

The shape recovery rate of 100% indicated a complete recovery to the original condition.

2.2. Statistical analysis

All data were expressed as the mean ± SD and were analyzed using the StatView version 5.0 software package (SAS Institute, Cary, NC). Statistical differences between the data before the separation and those after the separation were analyzed using the unpaired Student's t-test and checked by the Mann–Whitney U test. A probability value of < 0.05 was considered significant in all analyses.

3. Results

3.1. Change in the spinal cord length

The craniocaudal length of the spinal cord between C2/3 and C7/T1 was 55.5 ± 3.9 mm before the separation, and 50.1 ± 3.8 mm after the separation (Fig. 2). The spinal cord was shortened by 9.7% ($p < 0.01$).

3.2. Load-indentation relationship of the spinal cord

By increasing the load on the spinal cord, the spinal cord became flattened both before and after the separation. The maximum indentation at the load of 20 g was 2.06 ± 0.16 mm after the separation, which was similar to the maximum indentation before the separation (2.08 ± 0.26 mm) (Fig. 3). When the load was decreased from 20 g, the spinal cords became round and restored their shape. The final indentation at the load of 0 g (complete unloading) was 0.92 ± 0.16 mm after the separation and was statistically larger than that before the separation (0.76 ± 0.11 mm, $p < 0.05$).

3.3. Change in the shape recovery rate after the separation

The recovery rate was not significantly different between the separated and un-separated cords until 3 g (Fig. 4). At the load of 1 g, the recovery rate was 28.0 ± 2.2% before the separation and 23.6 ± 3.5% after the separation. At the load of 0 g, the recovery rate was 63.1 ± 5.9% before the separation and 55.5 ± 5.3% after the separation. The recovery rate after the separation was significantly lower than that before the separation at both 1 and 0 g ($p < 0.05$).

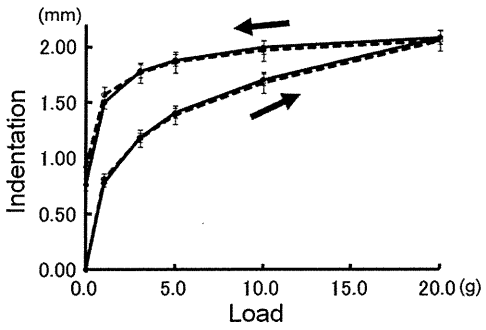

Fig. 3. Load-indentation relationship of the spinal cord during indentation test before and after the separation. By increasing the load on the spinal cord, the indentations of the spinal cord before the separation (solid line) and after the separation (dotted line) were similar. When the load was decreased from 20 g, the spinal cords restored their shape. The final indentation at the load of 0 g (complete unloading) after the separation was statistically larger than that before the separation. ($n=8$, mean ± SD).

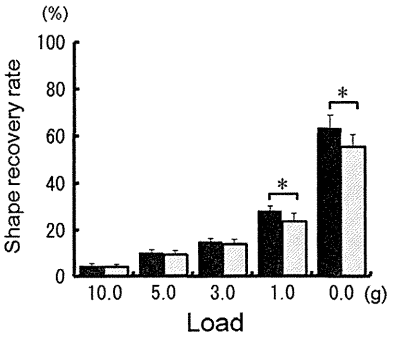

Fig. 4. Shape recovery rate after the separation (shaded bar) was significantly lower than that before the separation (black bar) at both 1 and 0 g. ($n=8$, mean $\pm$ SD, *p <0.05).

4. Discussion

Reid (1960) described that the length of the spinal dura mater and spinal cord were increased in flexion and that the average stretching between C2 and C5 was approximately 10%. Kuwazawa et al. (2006) reported that the mean elongation of the length of the cervical cord from extension to flexion was 11.7 mm in recumbent volunteers and 9.5 mm in erect volunteers on T2WI sagittal MR images. These values corresponded to 10.9% and 8.9% of the length in the extension position, respectively. In the present study, the spinal cord was placed in the straight position, and it was shortened by 10% after the separation. This value was in agreement with the aforementioned studies.

We described the factors causing shape recoverability of the spinal cord after decompression in cervical myelopathy (Ozawa et al., 2004). The decrease in the cross-sectional area of the compressed spinal cord during the acute phase likely results from displacement of interstitial fluid and cytoplasm in response to the Poisson effect (Panjabi and White, 1988). Shape recovery at an early stage after decompression may result from the movement of interstitial fluid from the periphery of the compressed site to the decompressed site. The spinal cord parenchyma exhibited viscoelasticity and an extremely low limit of elasticity (Ozawa et al., 2001). This indicates that the shape recovery of the spinal cord after decompression cannot occur by itself. The shape recovery must thus be induced by the strain energy in the spinal cord, that is, the intramedullary pressure (Tachibana et al., 1994). Iida and Tachibana (1995) demonstrated that the spinal cord intramedullary pressure is increased by mechanical compression on the anterior structure of the spinal canal and stretching of the cord in canine studies. Therefore, the tensile stress in the spinal cord can increase the intramedullary pressure and enhance the shape recoverability of the spinal cord.

In the present study, as the load on the spinal cord was increased, the stretch of the spinal cord did not influence the deformity of the spinal cord. The spinal cord did not seem to increase its stiffness by stretching. Bilston and Thibault (1996) showed that the spinal cord is initially compliant to stretch, and becomes progressively stiffer as the fibers straighten out and begin to bear tensile load. The physiological *in situ* stretch observed in the present study may therefore only slightly affect the stiffness and the deformity under compression.

These results indicated the basic properties of the spinal cord in the spinal canal. Although it was difficult to apply them to the clinical practices, the results assisted in understanding how physiological stretch was important to the shape recoverability of the compressed spinal cord in cervical myelopathy. Nagata et al. (1996) reported that the postoperative shape recovery of the compressed spinal cord was worse in aging patients compared to younger patients. Mechanical properties of neural tissue vary with age (Prange and Margulies, 2002). In addition to these changes induced by aging, the decrease in the physiological stretch and tensile stress of the spinal cord by shortening of the spinal column owing to intervertebral disc degeneration should contribute to the poor resilience of the shape after the surgery.

Conflict of interest statement

All authors have no conflicts of interest.

References

Bilston, L.E., Thibault, L.E., 1996. The mechanical properties of the human cervical spinal cord in vitro. Ann. Biomed. Eng. 24, 67–74.
Breig, A., el-Nadi, A.F., 1966. Biomechanics of the cervical spinal cord. Relief of contact pressure on and overstretching of the spinal cord. Acta Radiol. Diagnosis (Stockholm) 4, 602–624.
Iida, H., Tachibana, S., 1995. Spinal cord intramedullary pressure: direct cord traction test. Neurol. Med. Chir. (Tokyo) 35, 75–77.
Kuwazawa, Y., Pope, M.H., Bashir, W., Takahashi, K., Smith, F.W., 2006. The length of the cervical cord: effects of postural changes in healthy volunteers using positional magnetic resonance imaging. Spine 31, E579–E583.
Nagata, K., Ohashi, T., Abe, J., 1996. Cervical myelopathy in elderly patients: clinical results and MRI findings before and after decompression surgery. Spinal Cord 34, 220–226.
O'Shaughnessy, B.A., Koski, T.R., Ondra, S.L., 2008. Reversal of neurologic deterioration after vertebral column resection by spinal cord untethering and duraplasty. Spine 33, E50–E54.
Ozawa, H., Matsumoto, T., Ohashi, T., Sato, M, Kokubun, S., 2001. Comparison of spinal cord gray matter and white matter softness: measurement by pipette aspiration method. J. Neurosurg. 95 (2, Suppl.), 221–224.
Ozawa, H., Matsumoto, T., Ohashi, T., Sato, M., Kokubun, S., 2004. Mechanical properties and function of the spinal pia mater. J. Neurosurg. Spine 1, 122–127.
Panjabi, M.M., White 3rd, A.A., 1988. Biomechanics of nonacute cervical spinal cord trauma. Spine 13, 838–842.
Prange, M.T., Margulies, S.S., 2002. Regional, directional and age-dependent properties of the brain undergoing large deformation. J. Biomech. Eng. 124, 244–252.
Reid, J.D., 1960. Effects of flexion-extension movements of the head and spine upon the spinal cord and nerve roots. J. Neurol. Neurosurg. Psychiatry 23, 214–221.
Tachibana, S., Kitahara, Y., Iida, H., Yada, K., 1994. Spinal cord intramedullary pressure. A possible factor in syrinx growth. Spine 19, 2174–2178.

Spine

SPINE Volume 36, Number 22, pp E1427–E1434

BASIC SCIENCE

Induction of Autophagy and Autophagic Cell Death in Damaged Neural Tissue After Acute Spinal Cord Injury in Mice

Haruo Kanno, MD, PhD,*† Hiroshi Ozawa, MD, PhD,* Akira Sekiguchi, MD,* Seiji Yamaya, MD,* and Eiji Itoi, MD, PhD*

Study Design. Expression of light chain 3 (LC3), a characteristic marker of autophagy, was examined by immunohistochemistry and Western blot using a spinal cord injury (SCI) model in mice. Electron microscopic analysis was also performed to examine the anatomic formation of autophagy and autophagic cell death in the injured spinal cord.

Objective. To examine both biochemically and anatomically the activity of autophagy in the damaged neural tissue after SCI.

Summary of Background Data. Autophagy is the bulk degradation of intracellular proteins and organelles, and it is involved in a number of diseases. Autophagy can lead to nonapoptotic programmed cell death, which is called autophagic cell death. Recent researches have revealed the increased expression of LC3 and the anatomic formation of autophagy and autophagic cell death in damaged tissues of various disease models. However, previous studies have focused on apoptotic process but not autophagic activity as mechanism of neural tissue damage after SCI. To date, there has been no study to examine the expression of LC3 and the anatomic formation of autophagy after SCI.

Methods. The spinal cord was hemitransected at T10 in adult female C57BL/6J mice. The LC3 expression was examined by immunohistochemistry and Western blot. The anatomic formation of autophagic activity was investigated using electron microscopy.

Results. Immunohistochemistry showed that the number of the LC3-positive cells significantly increased at the lesion site after hemisection. The increase of LC3-positive cells was observed from 4 hours and peaked at 3 days, and it lasted for at least 21 days after hemisection. The LC3-positive cells were observed in neurons, astrocytes, and oligodendrocytes. Western blot analysis demonstrated that the level of LC3-II protein expression significantly increased in the injured spinal cord. Electron microscopy showed the formation of autophagic vacuoles to increase in the damaged cells. Furthermore, the nuclei in the transferase-mediated dUTP nick end labeling–positive cells expressed LC3 were round, which is consistent with autophagic cell death, and they were neither shrunken nor fragmented as is observed in apoptotic nuclei.

Conclusion. This study suggested both biochemically and anatomically that autophagy was clearly activated and autophagic cell death was induced in the damaged neural tissue after SCI.

Key words: spinal cord injury, autophagy, LC3, apoptosis, autophagic cell death. **Spine 2011;36:E1427–E1434**

Autophagy is the major cellular pathway for the bulk degradation of cytoplasmic proteins and organelles. This mechanism plays an important role in cellular homeostasis and it is involved in various diseases.[1–3] Previous studies suggested that autophagy has a cytoprotective function against cell death.[4,5] Autophagy contributed to cytoprotection in neurodegenerative disease and traumatic brain injury.[6–10] On the contrary, previous studies suggested that autophagy also contributes to the induction of cell death.[5,11,12] Autophagy can lead to nonapoptotic programmed cell death, which is called autophagic cell death.[13,14] A recent report showed the activation of autophagy to induce cell death in a myocardial ischemia and reperfusion model.[15] In addition, autophagy can lead to autophagic cell death in cerebral ischemia and in a renal ischemia and reperfusion injury.[16,17]

The molecular mechanisms of autophagy are being progressively elucidated from proteins initially described in yeast.[18] The mammalian homolog proteins are Atg proteins. The Atg8 protein, known as microtubule-associated protein 1 light chain 3 (LC3), is essential for autophagy. LC3 has a crucial function in the formation of autophagosome and thus is considered a specific marker protein to monitor autophagy.[19] LC3 is lipidated on activation of autophagy (LC-I, unlipidated;

From the *Department of Orthopaedic Surgery, Tohoku University School of Medicine, Sendai, Japan; and †Miami Project to Cure Paralysis, University of Miami, FL.

Acknowledgment date: July 27, 2010. Revision date: October 8, 2010. Acceptance date: October 18, 2010.

The manuscript submitted does not contain information about medical device(s)/drug(s).

Federal, Foundation, and Professional Organizational funds were received in support of this work. No benefits in any form have been or will be received from a commercial party related directly or indirectly to the subject of this manuscript.

Supported by Grant-in-Aid for Scientific Research (19591712) from Japan Society for the Promotion of Science, by Japan Orthopaedics and Traumatology Foundation, Inc. (No. 0138), and by Grant in 2007 from The General insurance Association of Japan.

Address correspondence and reprint requests to Haruo Kanno, MD, PhD, Department of Orthopaedic Surgery, Tohoku University School of Medicine, Seiryo-machi, Aoba-ku, Sendai, Miyagi, 980-8574, Japan; E-mail: kanno-h@isis.ocn.ne.jp

DOI: 10.1097/BRS.0b013e3182028c3a